Journal of Thermal Analysis and Calorimetry (2024) 149:1963–2006
https://doi.org/10.1007/s10973-023-12830-w

A comprehensive review of Trinitor components: A sustainable waste heat recovery polygenerative system for diesel vehicles

Balamurali Duraivel[1] · Saboor Shaik[1] · Ritik Bansal[1] · Shubhankar Debabrata Khanda[1] · Dhruv Patel[1] · M. Natarajan[1] · C. Ahamed Saleel[2] · R. D. Jilte[3] · Ümit Ağbulut[4]

Received: 28 July 2023 / Accepted: 9 December 2023 / Published online: 26 January 2024

Abstract

Internal combustion engine inefficiencies and waste heat emissions raise environmental concerns, as they waste fuel energy in the form of heat, increasing fuel consumption and greenhouse gas emissions. Additionally, waste heat contributes to the urban heat island effect. Waste heat recovery is a vital solution, capturing and repurposing heat to reduce fuel use, emissions, and costs while promoting sustainability, innovation, and economic growth. Polygenerative waste heat recovery maximizes energy efficiency by generating multiple forms of energy from a single source, enhancing overall sustainability. The proposed Trinitor model is a polygenerative system encompassing power generation, product drying, space cooling/heating, and oxygen production. Power generation utilizes exhaust heat stored in a phase change material (PCM) to generate electricity through a Hot Air Turbine. The PCM also stores heat from the PVT thermal collector and supports produce drying. In the space cooling/heating process, the temperature contrast resulting from the hot air generated by the turbine and the cooled air from the Cooling chamber is harnessed by the Seebeck principle within the TEG, converting heat energy into electricity, and it is possible to create temperature variations using the Peltier Effect by supplying electricity. Oxygen production involves dehumidifying air, separating oxygen from hydrogen using an electrolyzer and storing oxygen for civilian use. A component review identifies SiC wall flow-diesel particulate filters (DPF), a paraffin-based Latent Heat Storage System, and electric-assisted turbo compounding as cost-effective for energy production. Produce drying relies on hot air or infrared drying, a revolving wicks humidifier, and a cooling coil dehumidifier. Space cooling/heating needs a water-type PV/T collector, MPPT charge controller, lithium-ion batteries, and ceramic TEGs. A PEM electrolyzer with appropriate components (bipolar plates, electrodes, catalyst, membrane, and gasket) enhances oxygen production efficiency. Based on existing literature, the trinitor has the potential to attain an overall efficiency ranging from 40.12–54.81%. Thus, a combination of low-efficiency processes results in a highly efficient waste heat recovery Trinitor system, with further improvements possible through identified components' integration.

Keywords Waste heat recovery · Polygenerative system · Trinitor components · Diesel vehicles

Abbreviations

AC	Alternative current
AEV	All-electric vehicle
AETEG	Automotive exhaust thermoelectric generators
BDC	Bottom dead center
BIPV	Building integrated photovoltaic
CHAPS	Combined heat and power solar
CI	Compression ignition
CNT	Carbon nano-tubes
DC	Direct current
DLC	Double layered capacitor

✉ M. Natarajan
m.natarajan@vit.ac.in

✉ Ümit Ağbulut
umitagbulut58@gmail.com

[1] Department of Thermal and Energy Engineering, School of Mechanical Engineering, Vellore Institute of Technology, VIT, Vellore, Tamilnadu 632014, India

[2] Department of Mechanical Engineering, College of Engineering, King Khalid University, PO Box 394, 61421 Abha, Saudi Arabia

[3] Energy Centre, Maulana Azad National Institute of Technology (MANIT), Bhopal, M.P. 462003, India

[4] Department of Mechanical Engineering, Mechanical Engineering Faculty, Yildiz Technical University, Istanbul, Turkey

DPF	Diesel particulate filter
EAT	Electrically assisted turbocharger
EPDM	Ethylene propylene diene monomer
EPR	Evaporator and pressure regulator
HD	Heavy duty
H/D	Humidification-dehumidification
HAT	Hot air tubine
HDPE	High density polyethylene
HER	Hydrogen evolution reaction
HEX	Heat exchanger
HSPM	High-speed permanent magnet
ICE	Internal combustion engine
IR	Infrared waves
IRD	Infra-red dying
LD	Light duty
LDPE	Low density polyethylene
LHS	Latent heat system
LHTES	Latent heat thermal energy storage
LPG	Liquified petroleum gas
MD	Medium duty
MW	Micro-waves
NPG	Neopentylglycol
PAPBI	Phosphoric acid doped polybenzimidazole
PBI	Polybenzimidazole
PCM	Phase change materials
PEG	Poly-(ethylene glycol)
PEMFC	Proton exchange membrane fuel cell
PERT	Pentaerythritol
PFSA	Perfluorosulfonic acid
PG	Pentaglycerine
PGM	Platinum group material
PHEV	Plug-in hybrid electric vehicle
PM	Particulate matter
PV/T	Photovoltaic/thermal
PWM	Phase width modulation
RF	Radio frequencies
RH	Relative humidity
SHS	Sensible heat system
SHTES	Sensible heat thermal energy storage
S.I.	Spark ignition
SOEC	Solid oxide electrolyzer
SS-PCM	Solid-solid phase change materials
SWH	Solar water heating
TEG	Thermo-electric generator
TES	Thermal energy storage
TEM	Thermo-electric modules
TM	Transition metal
TPM	Total particulate matter
TRIS	Tris(hydroxymethyl)aminomethane
MEA	Membrane electrode assembly
MPPT	Maximum power point tracker
OER	Oxygen evolution reaction

Introduction

There has been a tremendous improvement in every part of society in the modern world. The production of electrical and thermal energy is driving this improvement in living conditions and human potential. The tremendous growth in energy demand over the past few decades has been met by fossil fuels. In 2018, renewables, nuclear energy, hydropower, natural gas, coal, and, oil accounted for 4%, 4.4%, 6.8%, 23.9%, 27.2% and 33.6% of global primary energy consumption, respectively [1]. However, in 2018, fossil fuels provided 84.7% of the world's primary energy demand. It is hoped that CO_2 emissions would be reduced by 37 gigatons per year by 2050 [2]. Nations and organizations are confronted with an energy tri-lemma, which combines concerns about energy affordability and economics with a goal for environmental preservation and guaranteed energy security. Addressing these three concerns at the same time has proven to be a challenging task for energy planners [3]. There is a distinct flow from the Middle East, West Africa, and Russia to the USA, Europe, and China in the global crude oil trade, which in 2019 reached a volume of 2239 million tons. Concerns about high crude oil dependence have been raised by the large gap between oil suppliers and oil buyers of the world. This has led oil-importing countries to improve efficiency, diversify oil supply sources, and promote renewable energies in order to lessen the impact of supply and price shocks, even if it is in an area that can't be changed, like military and defense [2]. Thus, a dire and urgent need for reform is required in automobile applications and every country in the world has already started working toward that direction.

The issue of waste heat in internal combustion engines and its environmental effects is a major concern in the automotive industry. Waste heat is the unneeded heat produced during engine combustion that is released into the environment through the exhaust and cooling systems. The following are some of the issues and environmental consequences linked with waste heat. Internal combustion engines are inefficient because they waste a significant amount of fuel energy as heat. This inefficiency increases fuel consumption and greenhouse gas emissions. For example, gasoline-powered vehicles convert just 20–30% of fuel energy into work, squandering the remainder as heat [4]. Inefficient engines use more fuel to produce the same amount of power, increasing prices and producing more carbon dioxide (CO_2) and pollutants, contributing to global warming and air pollution. The release of waste heat has an impact on the local

and regional ecology. Hot exhaust emissions can heat up cities, adding to the heat island effect. Waste heat release in cities can amplify the urban heat island effect, raising city temperatures and influencing air quality, energy consumption, and liveability. Engines require cooling systems, which consume energy to handle heat and so reduce overall efficiency. Cooling and exhaust systems are used to remove heat and generate noise, both of which have an impact on vehicle occupants and the environment [5].

Waste heat recovery stands as a crucial strategy that tackles both air pollution and energy efficiency issues [300]. It assumes a pivotal role in capturing and reusing heat that would otherwise be released into the environment. This method substantially reduces the necessity for additional fossil fuel burning, resulting in decreased greenhouse gas emissions and improved air quality. Waste heat recovery systems also enhance energy efficiency in various sectors like industry, power generation, and transportation by harnessing thermal energy that would otherwise go to waste. This leads to a reduction in the consumption of primary energy resources, which lowers costs and lessens environmental impact. Moreover, it aids in adhering to strict environmental regulations, offers cost savings to businesses and consumers, and contributes to resource preservation. Additionally, it fosters innovation in energy efficiency and clean energy solutions, paving the way for new industries, job opportunities, and economic growth. In summary, waste heat recovery is a multifaceted approach crucial for achieving a sustainable and environmentally friendly future [6]. Figure 1 shows the Environmental impact of waste heat and recovery methods.

Diesel engines have been recognized to play a vital function in automobile sector. In recent years, extensive research has focused on enhancing diesel engine performance and waste heat recovery by integrating various components. Here is a condensed overview of the traditional approaches such as thermoelectric generators, bottoming cycles, turbocompounding and heat exchangers used in engine waste heat recovery. These solutions are advantageous not only for huge vehicles, but also for the transportation sector as a whole. A thermoelectric generator (TEG) is a solid-state device that converts heat transfer into electrical energy by using conduction or semiconductor principles. TEG has a number of advantages, including its environmental friendliness, low noise level, lack of moving parts, and low maintenance

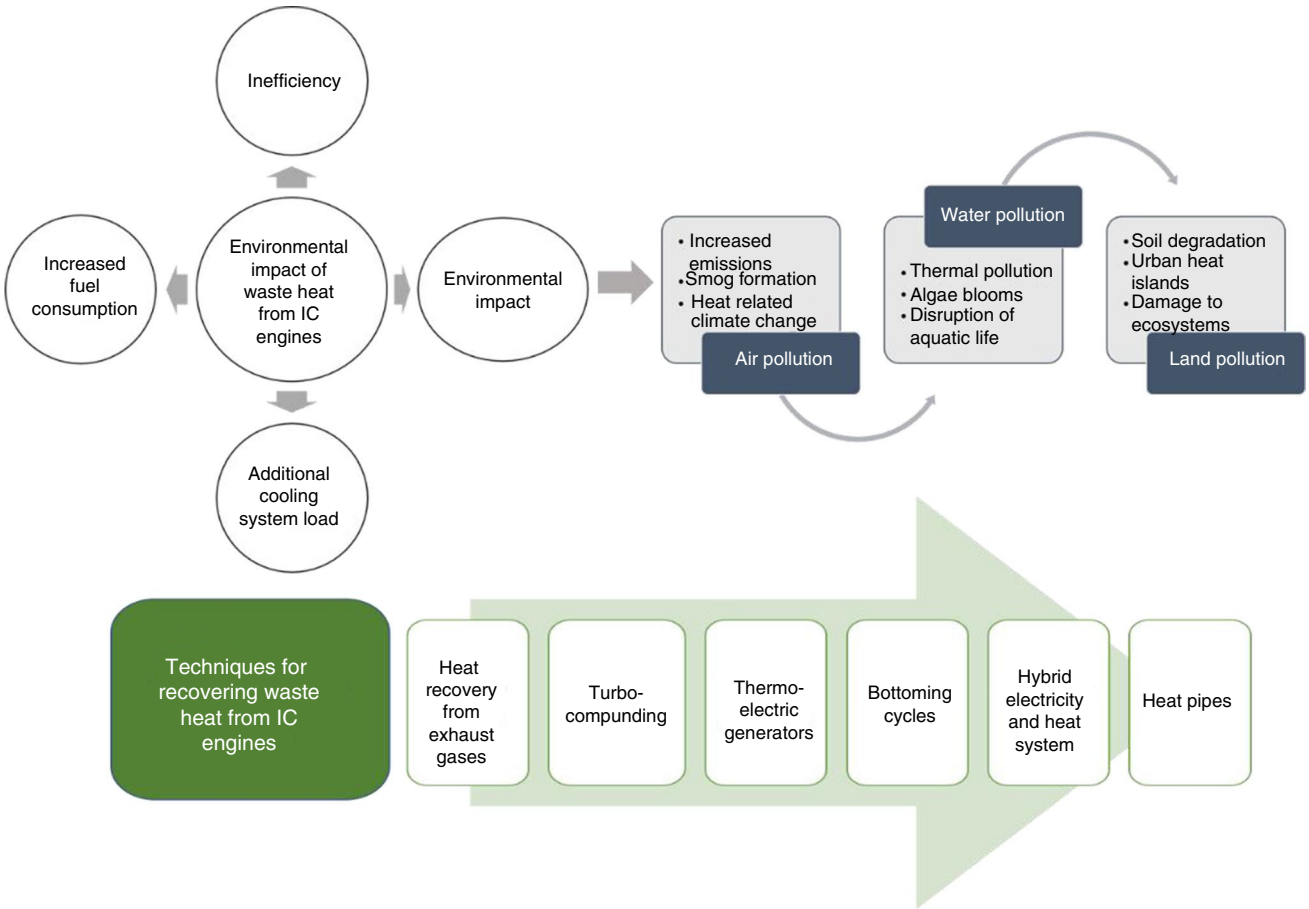

Fig. 1 Environmental impact of waste heat and recovery methods

costs. However, it only becomes economically viable when running at high temperatures with a limited power output. The authors conducted a mathematical model simulation to assess the performance of a TEG (TEP1-1264–3.4) in waste heat recovery (WHR). They used 126 modules operating within a temperature range of 248–396 °C and achieved a power output ranging from 185–605 W with an efficiency between 3.3–4.1% [7]. In another simulation, Y. D. Deng et. al applied 240 modules of Bi_2Te_3 TEG to 11.2 L diesel engine with an operating temperature of 115 °C, resulting in a power output of 995 W at 4.1% efficiency [8]. Furthermore, the authors conducted tests on TEGs (TG12-4) using a testing bench equipped with 100 modules at 125 °C, which yielded a power output of 130 W with an efficiency of 4.1% [9].

Waste heat recovery can also be achieved using secondary thermodynamic cycles called "bottoming cycles" to capture and use low-grade waste heat from primary energy operations like internal combustion engines and industrial processes. These cycles run at lower temperatures and pressures than the primary process to extract work or heat from wasted heat. Organic Rankine Cycles (ORCs), stirling cycles, and other heat-to-power systems aim to boost energy efficiency. Teng et al. conducted a simulation to recover waste heat from the exhaust gas of a Cummins ISX engine. They employed a T-type expander and a serpentine heat exchanger, with R245fa and ethanol as the working fluids. This approach yielded an efficiency ranging from 15.8–25.5% [10]. Cipollone et al. successfully recuperated waste heat from the exhaust gas of an IVECO NEF67 engine. They achieved this using a finned coil type evaporator and a T-type expander, and the working fluid of choice was R245fa. As a result, they were able to generate a power output in the range of 1–3 kW, exhibiting an efficiency between 9–0% [11]. Yutuc investigated the viability of integrating a Stirling engine into the exhaust system of a tanker's engine. The primary goal was to reduce fuel usage while also providing power for the dashboard. Although the Stirling engine model was not specified, they used a conventional cycle efficiency range of 20–50%. The Malmo formula was used to calculate the power generated by the Stirling engine [12]. Douadi et. al developed a mirror cycle that combines a cooled-inverse Brayton cycle with a multi-stage intermediate cooling technique. When compared to a standard gas turbine cycle, their research found that the mirror cycle can achieve significantly higher thermal efficiency [13].

Turbo compounding uses an additional turbine connected to the engine's exhaust system to recover energy from exhaust gases. This recovered energy is transformed into mechanical power to drive auxiliary equipment like electric generators or propellers in aircraft and ships. Heat exchangers are crucial to engine waste heat recovery. They are essential for transferring thermal energy from hot engine exhaust gases to other fluids or systems, enhancing engine efficiency and lowering energy waste. In their WHR experiment, Khordehgah et. al concluded that plate heat exchangers and heat pipe systems effectively transfer heat between sources with varying temperature ranges [14]. Table 1 lists some unique WHR methods reported. When comparing Trinitor to existing methods, it becomes evident that conventional approaches typically employ one technology at a time, resulting in a single output and relatively low efficiency in waste heat recovery. In contrast, Trinitor is a polygenerative process that encompasses power generation, cabin heating/cooling, product drying, and oxygen production. By combining two or more low-efficiency systems, Trinitor achieves a notable increase in overall efficiency. Therefore, Trinitor, as a polygenerative process, represents a highly efficient waste heat recovery technology.

A summary of notable studies on individual components aimed at achieving these goals is presented. Vehicle hybridization improves tactical capabilities by boosting available on-board power while lowering fuel costs [22, 23]. Due to increased power and energy density, as well as less cost, Li-ion battery technology is presently the most often utilized device for electrified systems [24]. Additionally, various energy storage devices can be added to enhance the vehicle's propulsion power [25]. Proton exchange membrane fuel cell (PEMFC) function at low temperatures, the cooling flow required is higher to compensate for the lower delta temperature between the air and the PEMFC. To help filter the load demand and support the power, fuel cell systems are frequently combined with a lithium-ion battery pack. The world is investigating the use of hydrogen as an alternate fuel. An electrolyzer can generate hydrogen fuel. Automotive Exhaust Thermoelectric Generators (AETEG) unit named "four-TEG system" made up of 240 thermocouples with a power output of 944 W was produced by Wuhan University researchers in 2014 [5]. The output of their TEG is believed to meet the electrical requirements of automobiles [26]. It was put on a military-purpose prototype vehicle called "Warrior" and tested at various speeds, with the findings indicating that the alternator may be replaced with an AETEG unit. Heat storage in vehicles can decrease vehicle setup time for tactical operations while serving as a protection mechanism [27]. Phase Change Materials (PCMs) may require much less mass to achieve the same heat capacity as a conventional heat storage system [302]. Energy density, melting and freezing point, and storage volume are all significantly lower for PCM than for non-phase-change solutions [28]. Thus, the power generated from the engine can be accumulated in a PCM storage tank.

Much research has been published on the subject of reducing diesel consumption and waste heat recovery with cutting-edge technologies. Individually, good work has been done on hybridization, energy storage, TEG utilization, and

Table 1 WHR methods reported

Sl. No.	WHR method	Objective	Description	Result	References
1	TEG	To create a TEG prototype that replaces an internal combustion engine's radiator	A 2.0 L diesel engine on an 80 km/h test vehicle was outfitted with 72 modules of TEG constructed of Bi_2Te_3 operating at 25 °C and with chilled coolant	75 W power output with 10% TEG efficiency and 0.4% overall efficiency	[15]
2	TEG	Energy recovery using TEG	A hybrid bus was simulated utilizing 96 TEG modules constructed of skutterudite operating at 266 °C and a heat sink cooling system	1926.7 W power output with 7.2% efficiency	[16]
3	ORC	WHR from 275 kW Cummins ISX engine	The heat source employed was exhaust gas, utilizing serpentine-type heat exchangers, and the working fluids included water, R134a, and R245fa	The power generated by the expander ranged from 50–55 kW and ORC efficiency was 29.5%	[17]
4	ORC	WHR from 12.7 L, 317 kW Euro VI US10 engine	They harnessed exhaust gas as the heat source, incorporating a plate-type evaporator and a *T*-type expander. The working fluid employed was a mixture of ethanol and water	The expander power output was 1–8 kW and ORC efficiency was 9–11%	[18]
5	Electric turbo compounding	Fuel economy	They harnessed the exhaust gas to generate electricity by rotating the turbine runner	The turbine is only capable of generating 1 W of power, determined by the runner's speed	[6]
6	Electric turbo compounding	Electricity production	Exhaust gas was utilized for electricity production	7% efficiency was achieved	[19]
7	Heat exchanger	Heat exchanger selection guidelines and their primary features	Plate fin and rotatory heat exchangers were tested	A higher compactness factor improves heat transfer and efficiency. Plate-fin heat exchangers have the highest compactness at 6000 m^2/m^3. Rotary wheel heat exchangers were found to be the most effective heat recovery system	[20]
8	Heat exchanger	Study on different heat exchangers	–	Supplementary factors that enhance the heat transfer rate and ensure thermal consistency in heat exchangers include the fin structure, the formation of the heat exchanger, and operational settings	[21]
9	Trinitor	To achieve power generation, oxygen production, cabin heating/cooling and drying by utilizing waste heat from exhaust gas	The Sustainable Trinitor model is a novel synergistic combination of multiple processes that work together to recover and reuse waste heat generated by the combustion of diesel engines in automobiles. It is a polygenerative system	Complete and multiple utilization of waste heat from exhaust The Trinitor system's overall efficiency in waste heat recovery will be substantial, given that it combines multiple low-efficiency waste heat recovery techniques	–

so on. However, research on the incorporation of a Polygenerative System (Comprising Electricity Production, Produce Drying, Space Cooling/Heating, and Oxygen Production) in automobiles is lacking. This paper is an investigation and selection of components required for the proposed sustainable conceptual polygenerative system model "Trinitor" for automobile applications. The average exhaust gas temperature of V-type diesel engines is in the region of 300–350 °C when they are idle. The Trinitor converts the heat from diesel engine's exhaust gas into electricity, cooling, and heating. In addition to the foregoing, an electrolyzer can be used to make hydrogen by water electrolysis. This system now includes a capability for supplemental power generation. Hydrogen and oxygen can be generated by the PEMFC using the electrolyzer's exhaust.

Novelty and objective of the present work

While diesel engine technology has come a long way, a lot of the fuel's chemical energy is still wasted as waste heat and exhaust. This is roughly the same as 30–40% of the energy that can be obtained from fossil fuels. Exhaust gas temperatures for diesel engines can be anywhere from 250–800 °C, depending on the engine model and the intended use. The entire focus of this work is on selecting the necessary elements for utilizing this thermal energy in automobiles via the proposed sustainable conceptual polygenerative system model "Trinitor" for a variety of purposes such as cabin heating/cooling, oxygen production, power generation, cooking and drinking water purposes. The proposed Sustainable Trinitor model is a novel synergistic combination of numerous processes that collaborate to recover, and reuse waste heat generated by diesel engine combustion in vehicles. To better understand the process, it is divided into four independent units: electricity production, produce drying, space cooling/heating, and oxygen production. The proposed procedure is shown in Fig. 2 as follows:

The simultaneous operation of all four units generates a large amount of electrical and thermal energy. Even with many more technologies across all four units that require electricity to function, this configuration is fairly self-sufficient in meeting demands and storing surplus energy as a backup. This entire process is extremely efficient and sustainable because it does not require any external energy source (other than renewable solar energy) and makes the best use of the waste heat generated. Different components are reviewed in this paper based on their application and usage in the Trinitor system. The proposed procedure has the following advantages:

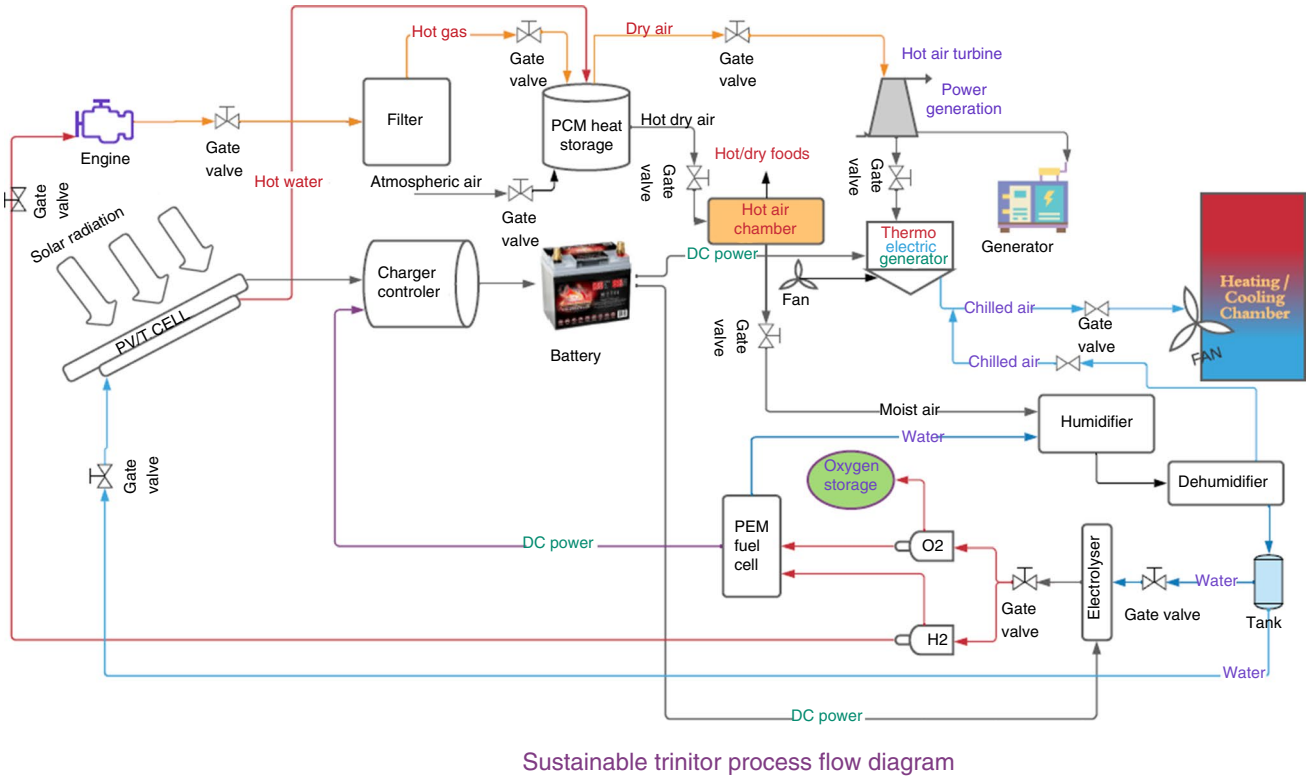

Fig. 2 Sustainable Trinitor process flow diagram

- Four different types of energy are used to power the vehicle and its sophisticated functions include a reduction in reliance on a single source (Solar PV) and providing backup energy at all times in the event of a problem.
- Cool or hot air can be produced from the cooling/heating chamber depending on demand; this is critical for vehicle comfort. However, cooling/heating is done in a separate chamber; it does not affect the vehicle's overall efficiency.
- Excess oxygen is stored in the vehicle, which is very important in times of medical emergency and can be accessed via a small bullnose wheel type valve, and bull nose regulator.
- Because the process has no rotating or moving parts (except HAT-Hot Air Turbine), it is entirely supported by thermodynamics, which increases the overall efficiency of the process.
- The use of solar panels in a vehicle takes advantage of sunlight and stores the energy for emergency usage.
- All of the parts are powered by direct current, there is no skin effect on the conductors, allowing the entire cross section of the conductor to be used, resulting in material savings and increased efficiency.
- Additional storage for hydrogen gases can be used as a gaseous fuel for the vehicle's engine.
- Energy-saving efficiency is a measurement that shows how much product or material is produced in the output from the input energy.
- Greenhouse gas emissions have been reduced.
- Furthermore, it has mobility, scalability, and controllability based on the needs of the end user.
- Under any circumstances, the process can be reversed. (Additional elevation, climatic, and seasonal conditions).

Electricity production

In this section and subsection, the methods used in Trinitor to produce electricity are handled. In this process, basically, heat generated from the engine exhaust is stored in a PCM storage and then is used for turbo-compounding using a hot air turbine. Accordingly, a schematic view of the electricity generation process in Trinitor is illustrated in Fig. 3.

Engine

Only a small fraction of the energy in exhaust gases is converted into electricity, and the process is permanent because of environmental and other considerations [29]. At temperatures above around 600 °C, exhaust gas emissions exceed 30% of the gas's energy value, but they decrease with increasing temperature [30]. Under light engine loads, exhaust gas emissions are minimal, but this is crucial for the motor's peak efficiency [31]. The required application calls for a diesel engine, which has been selected for this prototype model. Table 2 and Fig. 4. show vehicle exhaust temperatures and variables affecting them.

Some researchers have investigated the impact of exhaust backward pressure on diesel engines, for example, on ambient diesel engines in which the pressure difference exceeds the air pressure [33], on 2-stage diesel engines

Table 2 Types of vehicles and their temperature change in the exhaust emission [30–32]

Types of vehicles	Gas temperature
Light passenger car	500–900 °C
High-performance engines	400–650 °C
Marine engine	250 °C and 500 °C
Saab biopower car	400–600 °C

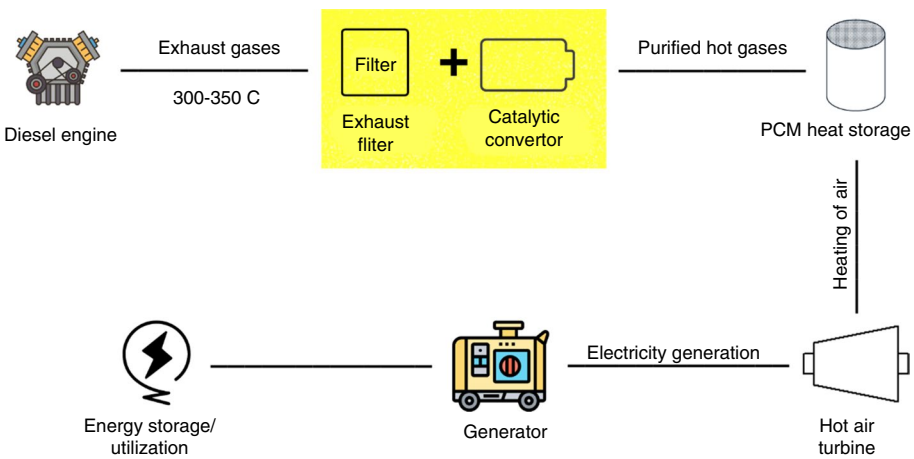

Fig. 3 The process of electricity generation

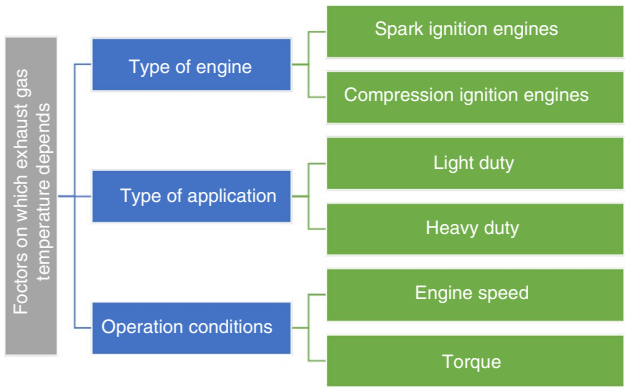

Fig. 4 Factors affecting exhaust gas temperature

with turbochargers, and turbo-compounding usage [34, 35]. Higher diesel engine exhaust back pressure has been determined to be the cause of increased negative pumping work. The increased pumping effort is neutralized by the current generated by the turbo-compound and also the system's total thermal effectiveness is improved with the adjusted exhaust manifold pressure.

Filter

In this section, the role of a filter, after the exhaust gases are released is discussed. The types of filters discussed are Diesel particulate Filter (DPF), Wall Flow Filters and Metal fiber filters.

Diesel particulate filter (DPF)

DPF is a ceramic cylinder with thousands of tiny parallel channels that extend in a longitudinal direction toward the exhaust of the engine. The porosity of these filters has been fine-tuned for efficient dust removal with little air resistance [36]. Figure 5 depicts the design parameters of the DPF.

DPF substrates

The substrate is the most significant component of a diesel engine filtration system. These filter materials typically collect particulate matter by interception, impaction, and diffusion, as well as holding the particulate matter until regeneration occurs [37]. Since there are many different uses for DPF, from light duty (LD) to medium duty (MD) to heavy duty (HD), the following factors must be considered while designing DPF so that it does not melt or shatter.

- Designing the DPF-Particle Matter (PM) loading and regeneration method must be done depending on individual usage and material limitations.

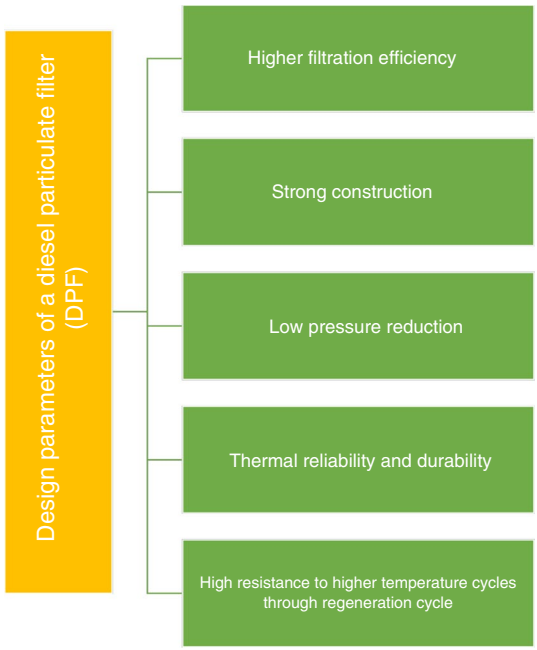

Fig. 5 Design parameters of a diesel particulate filter

- Competitive earthing equipment based on its characteristics must be chosen [38]. DPF substrates are shown in Fig. 6.

Wall flow filters

The most popular form of DPF substrate is wall-flow solid ceramic monoliths, developed from catalytic converters. They have a wide surface area per volume unit and a high degree of separation, which sets them apart from other DPF types [36]. Monolithic DPFs usually consist of several minute parallel channels that run axially through the element and are usually square in cross section. The following Fig. 7 depicts the important characteristic features of wall flow filters.

Cordierite and silicon carbide (SiC) are two minerals that are widely used in commercial filters [39]. Cordierite filters are widely known in heavy-duty diesel engine applications [41]. Aluminum titanate is a recent commercial monolith filter material that has been introduced. Figure 8a, b. shows some of the commercial manufacturers and suppliers of these monoliths.

SiC filter has high thermal efficiency, improved resistance due to thermal shock and thermal conductivity, and higher material strength properties [41, 42]. Due to its high coefficient of thermal expansion, a split design with a filter element is required. It is best suited for our applications which is why SiC filter can be incorporated in the Trinitor prototype [42]. Table 3 shows the characteristics and

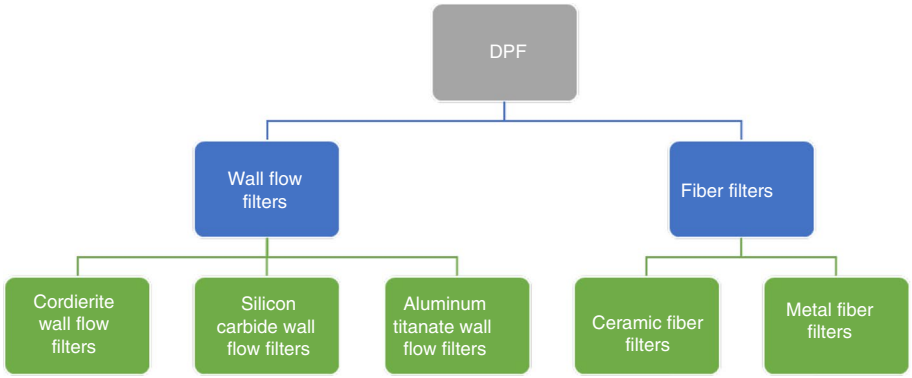

Fig. 6 Diesel particulate filter and their type of substrates

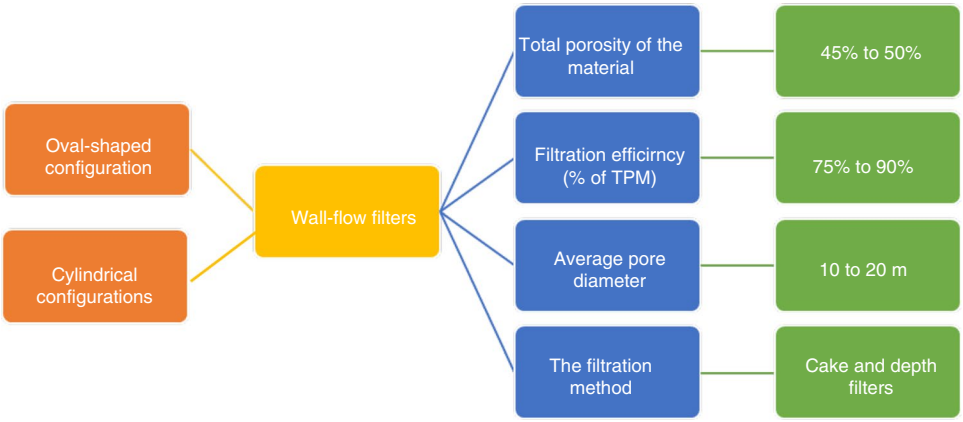

Fig. 7 Characteristic features of wall flow filters [39, 40]

characteristics of the various types of SiC substrates manufactured by NoTox [43].

Metal fiber filters

The main characteristics of metal fiber filters are shown in Fig. 9. All types of metal fiber composites can achieve up to 85% high porosity. Due to the high porosity of this media, relatively low back pressure is possible for most combinations [44]. Table 4 lists some of the most common commercial metal fiber filters and their parameters.

Heat storage

In this section, an analysis of the heat storage capability of different Phase Change Materials has been explored in detail. PCM materials are substances that have a considerably larger range of latent heat storage capacity and, hence are used to store heat.

PCM storage

Thermal energy storage (TES) with phase change materials (PCM) is a simple and practical technique to increase energy storage capacity and consumption in residential and commercial settings [46, 47]. The Trinitor model can make use of the thermal energy storage method of latent heat storage (LHS). Compared to sensible heat storage (SHS), LHS has a higher storage density and a narrower temperature range between heat storage and release, making it an effective way to store heat energy. Recent developments in the design and qualities of revolutionary energy storage materials, particularly micromaterials, have opened up new avenues for improved performance and longevity [48–50].

Types of PCM

Potential PCMs for low and high-temperature applications include a wide range of materials, eutectics, and compounds. Figure 10 shows various possible materials that can act as PCM. Tables 5, 6, 7 and 8 depict the thermophysical properties of various PCM types.

$KClO_4$ has the greatest melting temperature of 527 °C and the highest heat of fusion of 1253 J/g among inorganic PCM compounds [51]. Paraffins, fatty acids and their eutectic mixtures, esters, and other organic molecules all contribute to the makeup of organic PCMs. *n*-Hexaconzane among organic PCMs, has 26 number of carbon molecules, 56.3 °C and 256 J g^{-1} of melting temperature and heat of fusion, respectively [52].

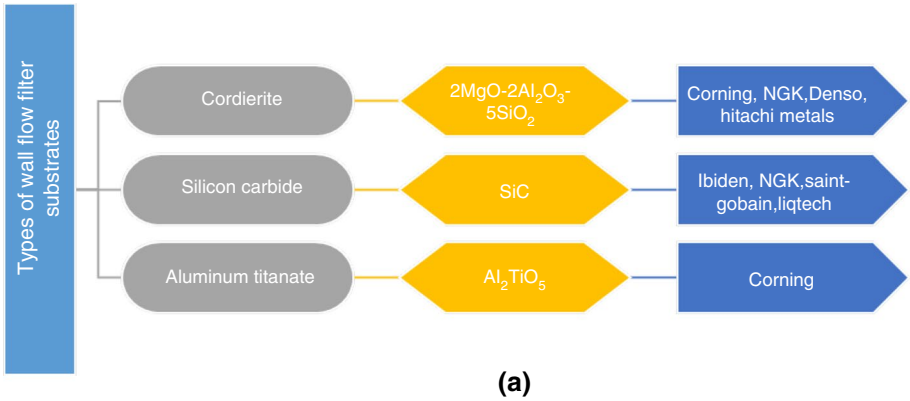

(a)

Types of substrates	Characteristics	Application
Improved cordierite	• Less expensive • More light-off properties	Light,medium,heavy-duty vehicle
Silicon carbide	• Expensive • High thermal efficiency • Improved resistance due to thermal shock and thermal conductivity • Higher material strength properties • Highe coefficient of thermal expansion	Light and medium-duty vehicles Best suited for military applications due to high temperature use
Aluminum titanate	• Newly developed for industrial applications	Passenger car

(b)

Fig. 8 **a** Types of wall flow filter substrates, their formula, and commercial producers **b** the characteristics and applications of the various types of wall flow filter substrates [41, 42]

Table 3 NoTox SiC model specifications and material properties [43]

Filter size—radius × length	R70 × 150	R95 × 205	R95 × 205	R95 × 205	R115 × 255	R125 × 205	R125 × 255	R160 × 255
Material (wall thickness-0.8 mm)	SiC	SiC	SiC	SiC	SiC	SiC	SiC	SiC
Mean pore size/μm	5	14.9	15.1	24.9	5.1	4.9	15	25.1
Open porosity/%	44.8	44.9	45.1	45	44.8	44.9	45.1	45
Max safe soot limit/g L^{-1}	> 10.1	6.1	> 10.1	6.1	8.1	6.1	> 10.1	> 10.1
Thermal conductivity/W m^{-1} K^{-1} at 25 °C	11.1	11.1	11.1	11.1	11.1	11.1	11.1	11.1
Thermal conductivity/W m^{-1} K^{-1}at 630 °C	6.99	6.99	7.1	7.1	7.1	7.1	7.1	7.1
Specific heat/J kg^{-1} at 25 °C	649.9	750	750.1	750.1	750.1	750.1	750.1	750.1
Specific heat/J kg^{-1} at 800 °C	1249.9	1249.9	1250	1250.1	1250.1	1250.1	1250.1	1250.1
Expansion/radial (× 10–6/°C) at 25 °C	420	420	420	420	420	420	420	420
Expansion/axial (× 10–6/°C) at 650 °C	390	390	390	390	390	390	390	390
Thermal shock parameter, TSP 3	160.0–1400.0	110.0–1100.0	110.0–1100.0	85.0–750.0	160.0–1400.0	160.0–1400.0	110.0–1000.0	85.0–750.0
Decompose/Melting temperature/°C	> 1800	> 1800	> 1800	> 1800	> 1800	> 1800	> 1800	> 1800

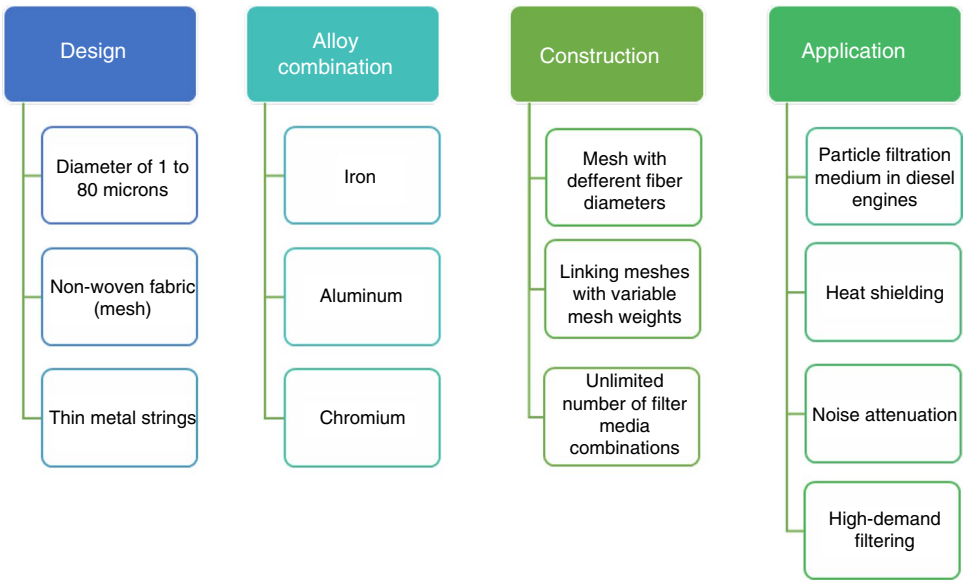

Fig. 9 Characteristics of metal fiber filters

Table 4 Few commercial metal fiber filters and their specifications [45]

Name	12 V	Regular	Mega	Super mega
Material	Fe–Cr–Al alloy	Fe–Cr–Al alloy	Fe–Cr–Al alloy	Fe–Cr–Al alloy
Porosity/µm	85	85	85	85
Media thickness/mm	1.34	1.34	1.34	1.34
Effective filter surface	0.12	0.5	1.0	2.0
Dimensions	133	48	292	292
OD/mm	60.8	60	115	115
ID/mm	130	260	140	263
H/mm				

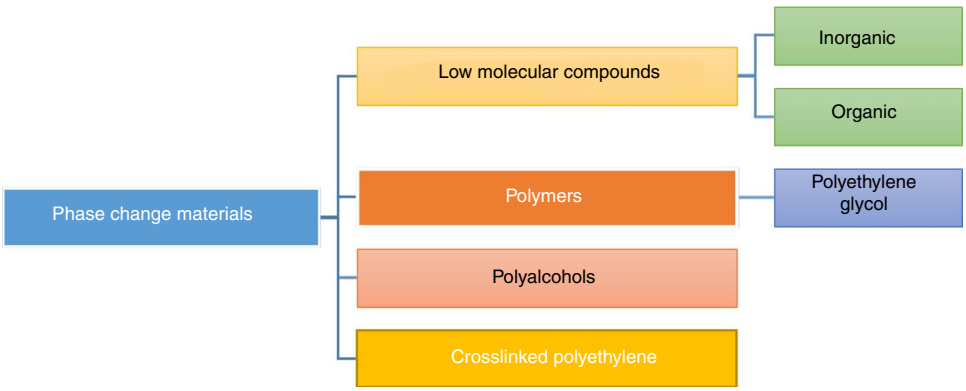

Fig. 10 Types of PCM

Polyethylene glycol (PEG) has a melting point, depending on the molecular weight, which ranges from 4–70 °C, with a heat of fusion of 117–174 J g^{-1}. It can be used as PCM because of its high fusion heat due to its crystallinity (83.8–96.4%) [61].

Polyalcohol can also be considered as PCM as it absorbs hydrogen bond energy at low temperatures and the temperature is raised to the solid–solid phase change threshold. For example, the transition phase temperature of neopentyl glycol (NPG) [$(CH_3)_2C(CH_2\text{-}OH)_2$] is 42–44 °C, and the heat of phase change is 110.4–119.1 J g^{-1} [64, 65].

PCM in the automotive industry

PCMs are used in the automotive industry for engine cooling systems, pre-heating catalytic converters, increasing customer comfort, and combustion engines [66]. Gumus used TES to reduce cold-start discharges from internal

Table 5 Inorganic PCM compound

Compound	Melting temperature/°C	Heat of fusion/J g^{-1}	References
$AlCl_3$	191.8	279	[53]
$LiNO_3$	251.1	371	[53]
$NaNO_3$	306.9	172	[28, 53]
KNO_3	334.2	265.9	[51]
$Na2O_2$	359.8	313.8	[54]
KOH	381.2	151.2	[28]
$KClO_4$	526.8	1252.8	[51]

combustion engines [67, 68]. Also, during cold start and increasing temperatures stages, pre-heating the engines minimized CO and hydrocarbon pollutants by 64% and 16%, respectively. This explained that PCM stores thermal energy to solve cold start issues in an LPG (Liquified Petroleum Gas)-fueled vehicle. After a waiting period, it was found that EPR (Evaporator and Pressure Regulator) with the addition of PCM to some extent reduces the cold start issue of LPG fuel engines [69, 70]. Heat storage in the accumulator is a unique approach that leads to a reduction in the engine cooling system [70, 71].

Because of their high heat of fusion, various phase change temperatures, little supercooling, the lower vapor pressure in a melt, and chemically inert and stable behavior, paraffin waxes have been widely employed for thermal energy storage [301]. They are also reasonably priced on the commercial market. These PCMs are also non-toxic

Table 7 Types of polymers PCM material

Polymer	Melting temperature/°C	Heat of fusion /J g^{-1}	References
PEG 400	4.4	117.4	[60]
PEG 600	12.7	129.2	[60]
PEG 1000	40.2	168.4	[61]
PEG 3400	63.6	166.6	[61, 62]
PEG 10000	65.7	171.8	[61, 62]
PEG 20000	67.5	160.4	[61, 62]
PEG 35000	68.9	166.7	[61, 62]
PEG 100000	67.2	175.6	[61, 62]]
PEG 1000000	70.4	174.2	[61, 62]

Table 8 Types of polyhydroxy alcohols

PCM	Phase transition temperature/°C	Heat of phase transition/J g^{-1}	References
Polyhydroxy alcohols			
Glycerine	18.4		[63]
Pentaerythritol	187–189	288.9–339	[64]
Pentaglycerine	84	173.1	[65]
Neopentylglycol	44–46	111.9–118.9	[64, 65]
Tris[hydroxymethyl] aminomethane	131.9–133.1	284.9–296.2	[64, 65]

Table 6 Types of organic PCM

Paraffin	Number of carbon atoms in the molecule	Melting Temperature /°C	Heat of fusion/J g^{-1}	Density/.g cm^2	References
n-Tetradecane	14	5.9–6.1	229–227	NA	[52, 55]
n-Pentadecane	15	9.8–10.2	208	NA	[56, 57]
n-Hexadecane	16	17–21	218–238	0.771	[52, 53, 55, 58, 59]
n-Heptadecane	17	22.2–22.8	163–215	0.776	[52, 53, 55, 58, 59]
n-Oktadecane	18	28.0–28.4	200–244	0.776	[52, 53, 55, 58, 59]
n-Nonadecane	19	32.3	221.8	0.783	[52]
n-Eicozane	20	36.5	247.2	0.786	[52]
n-Heneicozane	21	40.3	213	0.793	[52]
n-Docozane	22	44.2	249.1	0.792	[52]
n-Trikozane	23	47.4	233.8	0.798	[52]
n-Tetracozane	24	50.7	254.8	0.797	[52]
n-Pentacozane	25	53.6	238.1	0.803	[52]
n-Hexacozane	26	56.2	255.2	0.805	[52]
n-Heptacozane	27	58.9	234.8	0.777	[52]
n-Oktacozane	28	41.1	254.3	0.808	[52]
n-Nonacozane	29	63.5	238.1	0.806	[52]
n-Triacontane	30	65.3	252.3	0.773	[52]

and environmentally safe [49]. Due to the supporting factors, paraffin waxes can be utilized in the Trinitor prototype**.** Polyethylene (PE) supports form-stable PCMs because of its chemical affinity for paraffin [72]. Sari made paraffin/HDPE SS-PCMs (solid–solid PCMs) by melt mixing [73]. The greatest percentage of paraffin in the PCM composites for two distinct types of paraffin was 77%, nicely distributed in the solid HDPE matrix. In addition, graphite, expanded and exfoliated by heat treatment, improved the thermal conductivity by 14–24%. Krupa et al. [74] investigated composites of low-density polyethylene (LDPE) and soft and hard Fischer–Tropsch paraffin waxes [75]. Soft paraffin waxes co-crystallized with the LDPE crystals, creating a more compact blend than the Fischer–Tropsch paraffin wax. Macroscopically, the mixes efficient SS-PCMs with LDPE matrix, retaining a compact shape.

Future trends

Over the past two decades, all research articles have shown interest in thermal energy storage using PCM, a fast-emerging topic since 2016. The goal to limit electricity consumption's ecological impact, especially in pursuit of sustainable growth over the previous decade, may explain this tendency [76]. Nano- and bio-based materials will dominate PCM trends, nanomaterials allow the creation of innovative, high-performance composites. [77, 78]. PCMs for TES also reduce carbon footprints and chemists, materials scientists, and engineers are developing innovative PCMs with improved physical properties, particularly form-stable PCMs. Through improved thermal conductivity, such materials could alleviate the rate problem, reduce storage system size, and simplify production and encapsulation.

Hot air turbine & generator (turbo-compounding)

Turbo-Compounding is a methodology that employs a turbine and a generator in a vehicle to recover the waste heat losses in the exhaust gases released. In the following sections, a thorough study of different types of turbo-compounding implementations and their respective performances has been detailed.

Turbo-compounding (turbine and generator)

Many laws and regulations reduce pollution and fuel waste. 30–40% of fuel is squandered and released into the atmosphere. Thus, vehicle waste heat recovery research and demand have increased. Figure 11 depicts prominent waste recovery methods. This paper focuses on turbo-compounding due to its simplicity, small mass, and low volume, which allows for many real-world applications.

Turbo-compounding is the process of extracting excess waste energy from the engine's exhaust using a power turbine. An electric turbo-compounding or turbo-generator generates electricity when the power is coupled to the turbine's output generator [79]. Turbo compounded systems can recover 11.4–25.7% of exhaust energy. Thus, exhaust flow energy recovery becomes 3.7 kW. If linked to an electric generator, the extra power can be used to operate the vehicle's auxiliary. The combined system generates enough power to run the Trinitor prototype's lights, air conditioning, and other comforts.

Turbine

Turbo-compounding in diesel engines reduces brake-specific fuel consumption due to turbine efficiency. The tip radius and outlet blade angle of the turbine affect turbo-compound engine performance [80]. Commercial hybrid flow turbines for turbo-compound utilized in 1L turbocharged diesel engines have lower low-pressure ratio capabilities. However, this turbine achieved over 70% efficiency at 50,000 rpm, 1.08 pressure ratio, and 1 kW of output [81, 82]. Radial turbines mismatch exhaust energy pulses in high-pressure turbo-compound diesel engines with split exhaust manifolds. Converting turbine peak capacity to a lower blade-speed ratio improves engine thermal efficiency and exhaust energy consumption [83].

Generator

Most car waste heat recovery power generation systems use High-Speed Permanent Magnet Synchronous (HSPMS) generators. Researchers designed a 10 kW, 70,000 rpm super permanent magnet motor/generator for an electrical turbo-compounding system [84]. HSPM operation and sound in an Electric-Assisted Turbocharged (EAT) system were studied [84]. The slot-less toroidal wound motor outperforms two 6-slot machines of different slot widths in efficiency and noise [84, 85]. A surface-mounted permanent magnet motor for an electrically assisted turbocharger (4 kW and 150 rpm) was studied. According to engine development projects, boosting exhaust system pressure increases energy recovered in the turbo-compound and reduces energy lost to the blow-off pulse when the exhaust valve opens. A negative pressure differential between the inlet and exhaust manifolds increases exhaust manifold pressure and negative pumping effort. Adjusting exhaust manifold pressure improves thermal efficiency and balances pumping labor from the turbo-compound. This diesel engine turbo-compounding study is comprehensive. Waste exhaust heat provides 30–40% of the fuel's energy. Thus, every waste heat recovery system must recover energy to reduce fuel waste. Turbo-compounding is simple, low-volume, and light compared to other

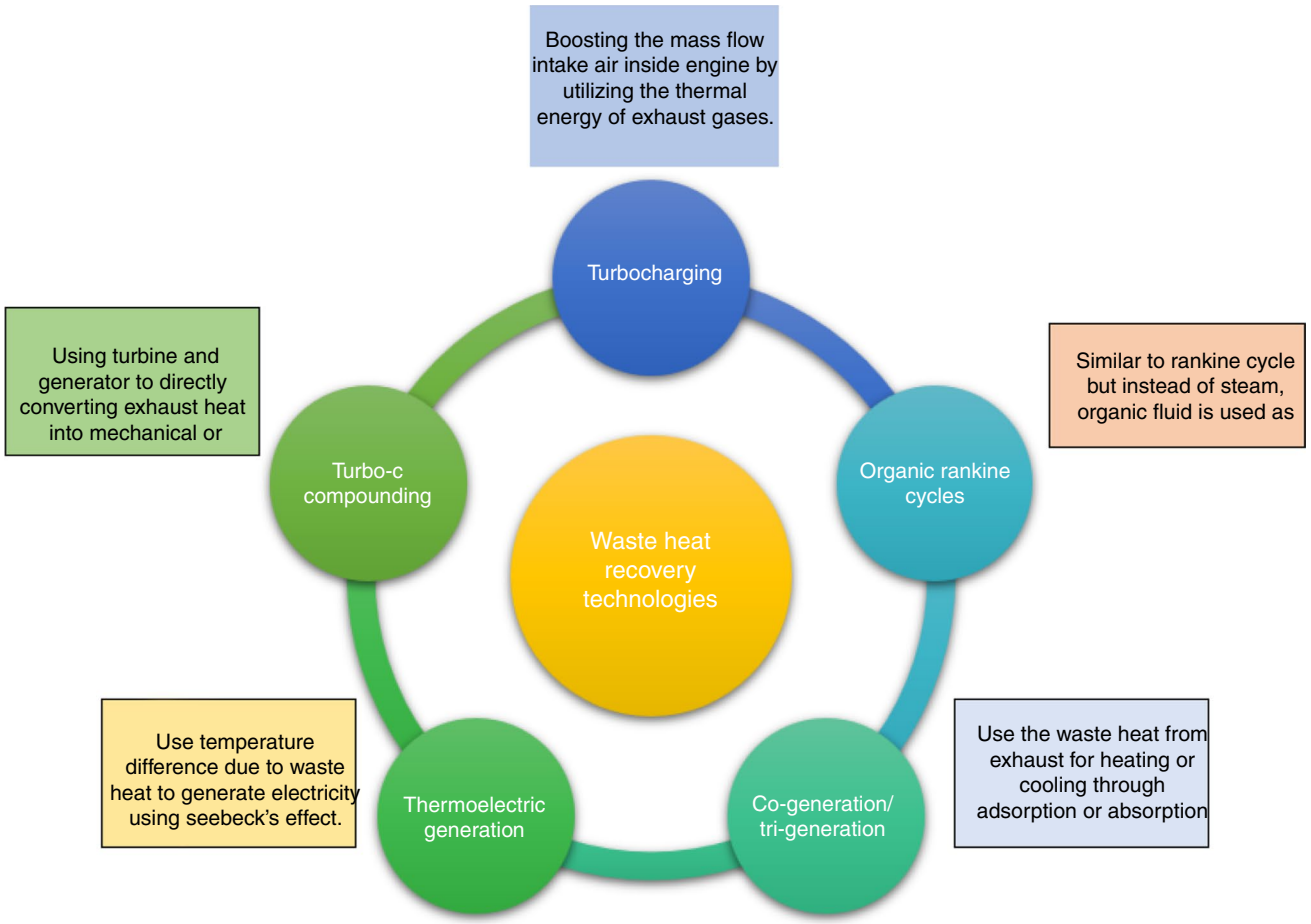

Fig. 11 Waste heat recovery methods

technologies. It also allows engineers to build engines for maximum efficiency. This study found that raising motor-boosted pressure in the turbocharger has improved it by 44.9% compared to the standard turbocharger [86].

Developments in turbo-compounding

Due to its simplicity and compact size, the turbine-generator combination for diesel engine exhaust heat recovery is appealing to many researchers. Power turbine characteristics, two-stage turbine interaction, and steam injection were studied on turbo-compound diesel engine performance. Steam injection and turbo-compound minimize fuel consumption by 6–11.2% at varied speeds [87–89]. Power turbine fluid flow, transmission ratio, and turbo-charged turbine fluid flow affect diesel vehicle capacity in a controllable, mechanical turbo-composing system. At 1600 r/min and 970 Nm matching points, the flow of a super-charged turbine 0.75 is estimated. The power turbine flow area coefficient is 1.6, the fixed ratio is 25, and fuel consumption can be reduced by 4.3% and 1.28% [90]. Mechanical turbo-compound has already entered the market and has been adopted by many commercial heavy-duty diesel engine vehicle manufacturers. Table 9 gives us an overview of some of these real-world applications.

Mechanical and electrical turbo-compounding can be improved and developed even when mechanical turbo-compound has become commercial. Table 10 shows new research on turbo-compounding on different engines and its feasibility with other automobile components like turbochargers and compressors to reduce fuel consumption and boost energy production.

Drying of produce

The heated air from the PCM storage can be used to preserve and maintain hygiene for food products. In this section, we discuss different methods of maintaining food hygiene and preservation using a Hot Air Chamber, also controlling moisture levels using humidifier and dehumidifier.

Table 9 Mechanical turbo-compounding in heavy-duty diesel engines [91]

Engine	Displacement/L	Power/Torque, kW/Nm	Benefit	Turbine
Volvo D13TC	12.9	371/2506	–	Axial turbine, ~ 39 kW
Daimler OM473	15.5	461/2999	–	Axial turbine
Volvo MD13TC	12.7	363/3049	–	Axial turbine
Detroit DD15	14.8	353/2239	2.5%	Axial turbine, ~ 26 kW
Volvo D12 500TC	12.1	329/2399	2.9%	Axial turbine, ~ 32 kW
Scania DT12	11.9	350/3058	–	Radial turbine
Scania DTC11 DTC12	11.7	294/1750	–	Radial turbine
Cummins NTC-400	14	334/2642	4.59%	Radial turbine, ~ 36 kW

Hot air chamber

A hot air chamber is a device which will be responsible for keeping food products warm for longer periods using various methods which are discussed in detail in the following sections.

Hot air dryer/chamber

High-temperature water evaporation modifies food's chemical, physical, and biological qualities simultaneously or sequentially. Shrinkage, textural distortion, discoloration, flavor loss, and surprising texture are the most obvious flaws in dried goods. Food drying degrades rehydration and nutritional quality [100]. (Commercial drying process shown in Fig. 12.)

Post-collection innovation has used the sun, osmotic, vacuum, hot air, fluid bed, and freeze-drying. Drying entails mass and heat conversion mechanisms that consume energy to remove moisture from food cells [102]. Traditional current drying methods can dry 1 kg of food with 14.53 MJ–90 MJ [103]. Accordingly, it is important to design energy-efficient drying to reduce the food safety cost and carbon impact of conventional electric dryers [104]. Table 11 lists hot air-drying experiments on agricultural products.

Combination of microwave and hot air drying

During a combination of microwave and hot air drying, convective air movement quickly removes microwave-heated moisture from the product surface without releasing energy into the atmosphere [115, 116]. This approach enhances drying rate, efficiency, and drying time substantially. Mostly, microwave radiation efficiency combines microwave and hot air to control production during drying, and leads to precise heating, which increases the drying rate, drying time, and yield of crops [117].

Combination of infrared and hot air drying

Infrared drying (IRD) uses electromagnetic radiation from 0.78 to 1000 m wavelengths. Infrared radiation is divided into close (0.78–1.40 μm), medium (1.40–3.0 μm), and far (3.0–1000 μm) wavelengths depending on the drying rate [118]. Infrared and hot air-drying together reduce power consumption and drying time, and increase heat and mass transmission [119]. Infrared and hot air-drying crops exposed to infrared radiation enhance molecular vibrations on the crop's internal surface layers, which accelerates moisture transport from the inner side of the substance. Convection air evaporates water vapor on the material's surface, lowering its temperature and improving the dry product [120–122].

Radio frequency and hot air-drying combination

Qualitative research on the combination of Radio Frequency (RF) (1–300 MHz's) and hot air-drying showed that, while quality declined, drying costs remained fair [123]. Also, when compared to air drying, there was a reduction in drying time. Energy consumption in this integrated process was only 40% of the individual energy needs [124]. The above Dryers suggest using use cabinet dryer or Infrared dryer in Trinitor. Table 12 lists combined system drying experiments of agricultural goods.

Humidifier

A humidifier is a device that disperses humidity into the air, which may be a requirement for dry climates and rooms with less moisture. In this section, we go through different types of humidifiers and their working in detail. The humidifier receives moist air from the hot air chamber, which is mixed with water from the PEM fuel cell before being transported to the dehumidifier. Chilled air is routed to the chamber from the dehumidifier. A humidifier can be a surface condenser

Table 10 Recent research work on turbo-compounding

Engine specifications	Additional turbo-compound/exhaust specifications	Comments/inferences	References
Heavy-duty 6-cylinder diesel engine	Exhaust gas recirculation in high- and low-pressure loops	Comparison of 1-stage and 2-stage turbochargers with rankine cycle turbocharging Turbocharging with Rankine cycle improved brake specific fuel consumption by 3%	[92]
2L diesel engine	Series Turbo-compound Power turbine behind turbocharger	Increase in engine's back pressure Turbo-compounding resulted in a 14 kW power gain	[93]
2L diesel engine	Parallel Turbo-compound Variable turbine geometry in turbocharger	Lower energy than series turbo-compounding Counterproductive at low load conditions Variable turbine geometry and reconfiguration of turbocharger give better outcomes	[94]
IVECO 3L diesel engine	Variable Turbine geometry in turbocharger	Better performance at low loads Power recovery of 2–2.5%	[95]
IVECO 3L diesel engine	Novel fixed geometry turbocharger	Better performance at high loads Power recovery of 2–2.5%	[95]
1L gasoline engine	Low pressure turbine turbo-compounding	Most effective in post-catalyst turbine position, in both low and high loading conditions 2.36% reduction in brake specific fuel usage and 2.2% improvement in brake mean effective pressure	[96]
ICE Diesel Engine (10 cylinder, 5.5L) Twin turbine turboshaft engine of power 500 kW	Turbo-compound with ICE engine	Comparison of turboshaft engine and ICE diesel engine ICE engine provided reduced fuel consumption and emissions The reduction in fuel consumption was about 25% to 50% compared to turboshaft engine	[97]
6 Cylinder, 4 stroke heavy-duty diesel engine	Electric turbo-compounding Series turbo-compounding Parallel turbo-compounding	Electric turbo-compounding provided the best power increase and the best reduction in fuel consumption Worst power increase and reduction in fuel consumption was of parallel turbo-compounding	[98]
1L Eco boost gasoline engine	Low pressure turbine for electric turbo-compounding	Maximum reduction in brake specific fuel consumption of 2.6% was achieved at 2500 rpm	[96]
13L Heavy duty diesel engine	Asymmetric twin scroll turbocharger	At medium speed and load, brake specific fuel consumption was lowered by 0.99% The transient operation of electric turbo-compounding with a bypassed valve reduced brake specific fuel consumption by 1.4%	[99]

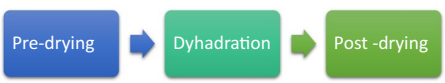

Fig. 12 Food drying process [101]

that uses chilled water, or it can be a humidifier that uses tubes to circulate humid air [131], whose types are shown in Table 13.

Types of humidifiers

Table 13 summarizes the types of humidifiers, working principles, advantages, and disadvantages.

Table 11 Studies on agricultural foods using hot air drying

Agri-product	Type of dryer/heat source	Temperatur/°C	Velocity/m s^{-1}	Activation energy/ kJ $mole^{-1}$	Refs.
Potato	Dryer for used heat	52–72	1.3	46.99 ± 0.03	[104]
Sweet potato	Conventional hot air dryer	49–69	1.9–4.1	29–36.98	[95]
Apple	Cabinet dryer	51–82	2.2	29.55	[105]
Apple	Thermal blast dryer, electric	42–64	1.19	24.61	[106]
Grape seeds	Convective hot air dryer	39–62	1.49	31.05–39.99	[107]
Pomegranate	Laboratory mechanical dryer	53–61	–	30.02	[108]
Tomato	Convective dryer	27–46	1.1–1.29	23.16–44.12	[99]
Olive	Convective dryer on a laboratory scale	19–83	1.2	16.78	[109]
Carrot	Electric forced convection dryer	62–72	0.6	22.04	[110]
Tomato waste	Mixed-mode solar tunnel dryer	52–84	0.6	36.44	[111]
Onion slices	Infrared convective dryer	37–43	1.2–1.7	5.04–10.6	[112]
Carrot	Infrared dryer	51–81	–	22.53	[113]
Carrot	Cabinet dryer	49–69	1.2	28.29	[114]

Why we choose a revolving wicks type humidifier?

Evaporative humidifier wicks collect minerals and other impurities in water. The wick keeps this chemical from entering your air. Evaporative humidifiers improve allergy and asthma symptoms in medical trials. The wick humidifier absorbs water from the force and dematerializes over a broader facial area. The addict blows air across the wick to evaporate water. Moisture affects wick evaporation. This humidifier automatically reduces water vapor production when room humidity rises.

Applications of humidifier

Music rooms, museums, and galleries can employ humidifiers to preserve paintings and instruments. Public and industrial buildings use air humidification to maintain humidity. Humidifiers are needed in freezers to prevent food from drying out. Static difficulties affect packaging, printing, paper, plastics, textiles, electronics, vehicle manufacturing, and medications. Friction can generate static buildup and sparks at RH below 45%. Static arises between 45 and 55% RH, but never above 55%.

Dehumidifier

A dehumidifier is a device that reduces humidity from the air, which may be a requirement for moisturized climates and rooms with higher moisture levels. In this section, we go through different types of dehumidifiers and their working in detail.

Dehumidifier

Dehumidifiers lower and maintain air humidity. This is done for health, thermal comfort, musty odor removal, and mildew prevention by extracting water from the air. Dehumidifiers should lower air moisture to 30–50% relative humidity [132]. Figure 13 shows a dehumidifier enthalpy diagram. A dehumidifier enthalpy graph visually depicts how the enthalpy of air changes during dehumidification. It shows the transformation of incoming humid air into drier air, with lower enthalpy values. This graph is essential for assessing the dehumidifier's efficiency and understanding how air properties change in the process.

Need of dehumidifier

RH is set in the dehumidifier's control system and the control system switches off when RH reaches the desired level. When the environment reaches a pre-set RH, the device restarts, repeating the cycle to ensure that your environment is never below prescribed RH values and that it is not wasting energy by running continuously [133]. Dehumidifiers maintain airflow by blowing dry, conditioned air to where it's needed, eliminating the need for ventilation.

Cooling coil type dehumidifier

This type dehumidifiers fit our Trinitor and a fan-assisted filter removes room air. An evaporator coil cools the filtered air below its dew point. Dehumidifying air condenses when the temperature drops below the dew point [134]. The

Table 12 Novel heating techniques used for agricultural products

Combination of technologies	Agricultural Products	Temperature/°C	Radiation	Air Velocity s^{-1}	Inferences	References
Microwaves + hot air drying	Lemon	50–60	185.5 W and 388.5 W	1.5	When contrasted to the hot air-drying method, the drying time was lowered by 20–30 times	[125]
	Oranges	55	200W	2.5	There was loss of moisture significantly faster than that of just hot air dryers	[116]
	Broccoli stalk	40–60	100W	1.4	The drying time of the combined system was reduced by 42–55% relative to conventional drying	[117]
	Papaya	40–60	180–900 W	0.8–1	Decreased drying time	[126]
Infrared + hot air drying	Apples	60	2000 W m	0.6	57.5% reduction in drying time was observed. Combined efficiency was observed to be 57.76% compared to 10.8% in the conventional method	[127]
	Chilli	50–70	2.4–3 µm wavelength of IR	–	Conventional hot air dyer used 33.5% more power than the combined system	[120]
	Corn	45	800 W	1	When compared to individual technologies, the integrated system has a lower specific energy usage and a higher carotenoid content	[128]
	Mushroom	40–60	0.49–0.22 W m	5	An increase in irradiation led to a decrease in drying time	[129]
Radio frequency + Hot air drying	Macadamia nuts	50–60	5.6 kW	1	The stoppage time increased quickly and then decreased swiftly. The drying curve, which frequently follows a regular descriptive fall, depicts the transfer of an internal mass within the material	[123]
	Tea leaves	118–122	16 kW	–	The combined energy use was only 40% of the hot air-drying energy demand	[130]

Table 13 Types of humidifiers

Sl. No.	Type of humidifier	Working	Advantages	Disadvantages
1	Humidification by injecting the steam	The humidification process is accomplished by infusing steam into the air flow. Steam immediately evaporates into gas. Thus, the relative humidity of the air rises without a temperature change. When a large amount of steam from the boiler is accessible or a discrete steam generator (boiler) is installed, several sorts of humidifiers are used	Low preliminary charge Free from unsafe impurities Soundless in operation	It carries a bad odor too with Increase in air temperature
2	Revolving wicks type humidifier	Air hits a rotating barrel in which woolen wicks are uniformly spaced. Drum harborage is always underwater and pier stopcocks balance water in the charger. The bath wicks evaporate the water as the barrel turns. Moisture-laden air is combined. The wicks spread water as the barrel grinds the water patches and thus humidity increases	It is easier to install than bypass types, requiring only a solitary cut hole for the installation, and requiring no added ducting It consumes very less electricity It will capture all the minute particles in the wick from air	Need to replace wick frequently
3	Atomization type humidifier	This humidifier is mostly used in industries with free compressed air. In the convergence zone, compressed air has high velocity and kinetic energy. Increased kinetic energy reduces pressure energy. High air velocity makes this humidifier noisy	It is a small, compact unit that can go where other sorts cannot It does not jeopardize the pressure separation (hence the efficient blower) of the return and delivery pipes as it does not require bypass ducting Water is used in an extremely efficient manner. It does not produce dirty water and does not require a separate drain connection	In hard water settings, the spray nozzle might become blocked, requiring the usage of a hydro-filter, regular nozzle washing, or a nozzle replacement Minerals present in water are dispersed into the air
4	Humidification by evaporating the water (shallow and pan coil type humidifier)	The water visage's heating system activates when humidification is needed. The water face vaporizes when an electrical coil, brume coil, or water heating coil heats the water. Depending on its surface area, air speed, and mixing water evaporates at varying rates. In a brume-heated humidifier, a huge, shallow body of water heats the brume coil. Water temperature depends on brume supply air is passed over water surface	It is easy to use There are no moving parts, therefore maintenance costs are negligible	Since the water has to be heated before the humidification begins and cooled before it ends, this humidifier does not allow for precise control of relative humidity

Table 13 (continued)

Sl. No.	Type of humidifier	Working	Advantages	Disadvantages
5	Humidification by air washing	This humidification method is the most popular and effective. Snoots allow water lines (banks of water sprays) to detect rapid water spouts in air. A little pump distributes high-pressure water to the spreading snoots. Air washing lowers air temperature. A heating coil is installed in the humidifier's bay. Part of water dispersed into the atmosphere evaporates, raising water vapor concentration and air moisture. Humidification uses discolored water. The force line's pier control stopcock controls water sump level. After sprays, water eliminator plates remove water driblets	Air can be made to leave moisture at any required temperature and relative humidity by calibrating the amount and temperature of the water passing through nozzles Relative humidity and temperature can be precisely controlled It is easy to use Low-cost maintenance	The spray nozzle may be clogged in hard water conditions, requiring the use of a water filter, periodic cleaning of the nozzle, or replacement of the nozzle

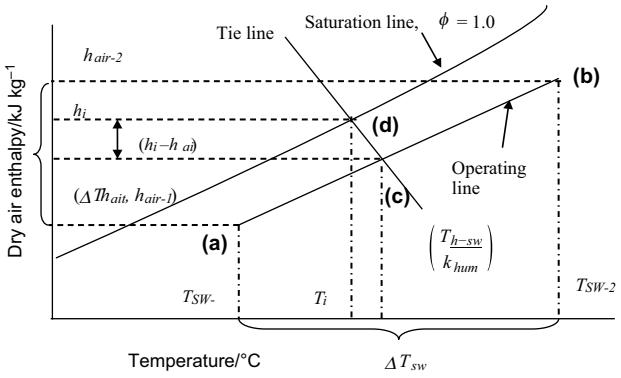

Fig. 13 Enthalpy diagram for dehumidification

condensed vent forces retrieved condensed water. The dehumidifier's humidistat measures humidity [135]. Dehumidifier selection is shown in Table 14.

Humidification—Dehumidification

Humidification–Dehumidification (H/D) is a process that produces freshwater by loading a carrier gas, usually air, with water vapors till saturation. H/D uses forced fluid circulation to humidify and dehumidify in two chambers. [136].

Applications

Pharmaceutical, food and drink, cold storage, waterworks and utilities, lithium battery manufacture, nuclear, automotive, aviation, chemical processing, car storage, archives, and wind farms use dehumidifiers. A dehumidifier, in essence, is an effective solution for practically any place that requires humidity control [133].

Space cooling/heating

After stabilizing the charged controller, the addition of a Photovoltaic Cell (PV) that catches solar radiation helps to maximize the potential for generating and storing extra electrical energy. The device thermo-electric generator (TEG) makes use of the "Seebeck's Effect concept" (TEG). According to this theory, the temperature difference between two dissimilar electrical conductors or semiconductors causes a voltage difference, which produces electricity. TEG is a collection of similar semiconductors connected in series to maximize overall output current. Following humidifier treatment, the chilled air from the Cooling chamber delivers the required temperature reduction. TEG converts heat energy to electrical energy, which can be used immediately or saved for use in future circumstances. Furthermore, we can induce temperature

Table 14 Application suitability table

Small spaces such as cupboards (under $10m^3$)	Peltier	Air circulation	Hot gas	Granules	Desiccant wheel
	R	S	S	R	S
Rooms with 0°–8 °C ambient temp	–	–	–	–	R
Rooms with 5°–35 °C ambient temp	–	–	R	–	S
Rooms with 15°–35 °C ambient temp	–	R	R	–	S
Construction	–	C	C	–	C
Flood damage	–	–	C	–	C

R = Recommended, S = Suitable, – = Unsuitable, C = Commercial/industrial types only

Fig. 14 Work focus

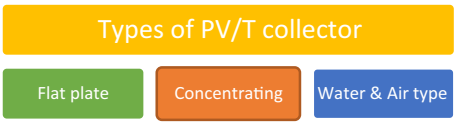

Fig. 15 Types of PVT collector

differences by giving the requisite power, which is the inverse of Seebeck's effect (also known as Peltier's Effect).

PV/T Panel

A photovoltaic-thermal solar panel is responsible for capturing both electricity and heat from solar energy. We use a PV/T panel in Trinitor as it provides another source of power and the heat captured can be stored in the Latent heat storage. In this section, we discuss many types of PV/T panels, their applications, performance, and work in much detail.

Solar PV/T panel

Renewable energy sources currently meet 13.5% of the world's key energy demand, with great future potential [137]. Different methodologies are used in the current study to reveal the classifications of PV/T hybrid solar collector systems. It also includes the primary applications used in the system under review. New technologies, such as the integration of TEGs into the PV/T system, are also being tested. The center of the effort is depicted in Fig. 14.

Types of PV/T collector

Figure 15 depicts the many types of PV/T collectors. Flat plate PV/T collectors have the same appearance as flat plate thermal collectors. The only obvious difference is the PV panel mounted on the upper side of the metal absorbent plate [138]. Focused or concentrated PV/T collectors use concentrators to improve the amount of irradiance reaching PV modules. Brogen et al. investigated the cold water-focused PV/T collector for the integrated structural type. PV/T series modules are used in conjunction with low-cost aluminum foil screens that have a dual concentration of 4.3 [139]. Coventry invented the "CHAPS" (combined heat and power solar) PV/T collector, consisting of monocrystalline silicon cells, with a two-axis tracking system and a parabolic trough with a concentration ratio of 37 [76]. To capture the majority of the heat produced, a water pipe and ice breaker were attached to the back of the cells.

Water type PV/T collectors are classed based on water flow pattern. They are classified as sheet and tube, channel, free flow, and two forms of stretch [140]. The air flow pattern also reflects the air conditioning PV/T collector.

Water type PV/T system

Water type PV/T system uses water as the working fluid medium for its operation. We discuss, the performances and utility of different types of PV/T – water systems.

Hendry and Raghuraman thoroughly examined the performance of the hybrid PV/T collector [141]. The tests are conducted outdoors, with varying quantities of intake fluid and weather circumstances, the thermal losses and efficiency coefficients obtained was 6.77 W mK^{-1} and 0.62, respectively [142]. Lalovic created and tested an amorphous silicon PV/T collector (a-Si). The overall surface area of the Si-PV cells employed in the investigation was 0. m^2 and the efficiency was average. According to test results, the hybrid PV/T collector performs better as a heat collector, heating water to a temperature of 65 °C. On the other hand, the system's electrical performance hasn't changed significantly. In

Table 15 Types of PVT-water systems

Sl. No.	Type of system	Electrical efficiency/%	Thermal efficiency/%	References
1	PVT-Water	9%	44%	[145]
2	PVT-Water	7.2%	54%	[146]
3	PVT-Water	9.7%	66%	[147]
4	PVT-Water	–	–	[148]
5	PVT-Water	–	–	[149]
6	PVT-Water	–	–	[149]
7	PVT-Water + Air	11–12%	80%	[150]
8	PVT-Water	11–16%	30–70%	[151]
9	PVT-Water + air	11–12%	40–55%	[152]
10	PVT-water	9–10%	–	[153]
11	PVT-Water	11%	50%	[154]
12	PVT-Water	14.2–15.5%	50–70%	[155]
13	PVT-water + air	9–10%	30–50%	[156]
14	PVT-Water	–	–	[147]
15	PVT-water	–	–	[157]
16	PVT-water	6–9%	40–75%	[158]
17	PVT-water + Heat pipe	9.4%	41.9%	[159]
18	PVT-Water + PCM	–	–	[160]
19	PVT-Water	–	–	[161]
20	PVT-Water	4–5%	23–27%	[161]

early 2010, many researchers sought to create hybrid PV / T water collectors [143, 144]. systems. Table 15 describes many types of PVT-water systems. PVT-water with 14% electrical capacity and 60% thermal efficiency will be suitable for Trinitor process.

Thermoelectric generators in PVT system

Photovoltaic thermal systems use TEGs to increase solar energy use. TEG generates electricity via the Seebeck effect and improves the electrical system conversion efficiency. This method works better for rooted systems since it provides more electricity at greater temperatures [149]. TEGs' no-moving-parts and compactness are advantages. The autonomous systems create far less energy [162]. The basic architecture is PV modules with TEG modules attached as illustrated in Fig. 16. The TEG module's cool side has a finned heat sink that cools the TEG and PV.

The advantages of TEGs are numerous like:

- Direct energy conversion, unlike heat engines that convert thermal energy into mechanical energy and employ an alternator to generate electricity.
- Maintenance is unnecessary because the TEG has no working fluids or moving parts.
- A prolonged life, particularly when working with continuous heat sources.
- Quiet operations.

Future trends of PV/T collectors

Table 16 shows some likely future trends in some markets for PV/T systems, which could become crucial to the renewable energy industry worldwide [164]. To attain the goals, more research is needed.

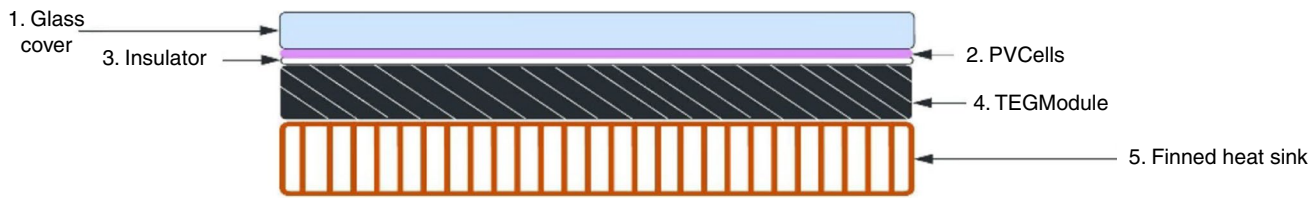

Fig. 16 Schematic diagram of PVT-TEG

Table 16 Possible future market segments of PVT

Market segment	Applications of PVT
Domestic market	Single and multi-family homes Apartment buildings
Market for service building	Hotels healthcare facilities and hospital office structures
Recreation industry	Aquatic facilities vacation bungalows sporting events
Farmer's market	Crop drying Stock breeders desalination

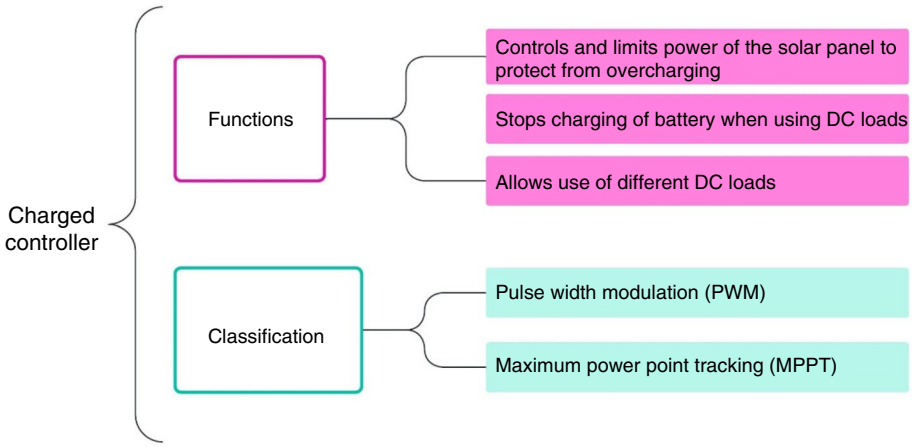

Fig. 17 Solar charge controller functions and types

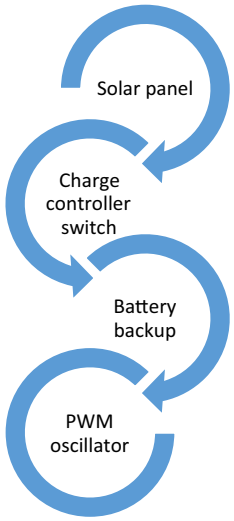

Fig. 18 Solar PWM charge controller's diagram

Charge controller A charge controller is a device that is used to regulate the voltage and current from the PV panel array to the battery. It is responsible for preventing overcharging and excess discharging from the battery. In this section, we discuss the types of charge controllers and their performance characteristics. A schematic understanding of the charge controller is shown in Fig. 17.

Modern high-performance battery chargers use PWM charge controllers (Fig. 18). PWM pulsing has various advantages, including 1. Locating and de-sulfating a misplaced battery, 2. Dramatically boost battery charge acceptance, 3. Maximum battery capacity, 4. Equalize wandering battery cells, 5. Reduce heat and gas emissions.

Eftichios Koutroulis et al. developed a new MPPT system with a microprocessor-controlled buck DC/DC converter [163]. The recommended MPPT system used PV output power to directly regulate the DC/DC converter, simplifying the system. The system is more efficient, cheaper, and adaptable to varied power sources (e.g., wind generators). The MPPT controller increases PV output power by 15% compared to DC/DC conversion cycles to reach a peak energy of 1 kW m and 25 °C [164].

MPPT will detect high solar radiation entering the PV module and create high power. As a result, it generates standard system costs [165]. In some circumstances, MPPT charge control is employed to dispose of the PV module's energy to form a'high power point' [165]. Tables 17 and 18 compare PWM and MPPT pros and cons. Trinitor can use only MPPT charge controllers to boost PV/T system output by 30%.

Battery In this section, a thorough review on different types of batteries suitable for various applications are discussed along with their applications and performance. The kind of battery used may differ depending on whether the vehicle is powered by an All-Electric Vehicle (AEV) or a Plug-in Hybrid Electric Vehicle (PHEV). Present battery technology aims for 8 years lifespan [169]. Some batteries endure 12–15 years in a chilly atmosphere and 8–12 years in a solid environment. Lithium-ion, nickel-metal hydride, lead-acid,

Table 17 Advantages of PWM and MPPT

PWM	MPPT
Triedand-true technology approves PWM controllers [165]	Solar charge controllers with MPPT technology can boost efficiency by up to 30% [166]
These controllers are low-cost [165]	MPPT units are more expensive than PWM because of their large body size
PWM controllers are available in a range of capacities ranging from 10 to 60Amps [165]	You can use a higher input voltage array with these controllers than you would with a battery bank [166]
PWM controls last longer, and many come with a built-in cooling sink [165]	It corrects solar cell I-V fluctuation during reception [166]
High current and voltage can be controlled [165]	It compels Photovoltaic panels to run at voltages close to their peak power in order to harvest the most available energy [166]
The projected lifespan is expected to be longer [165]	Reduces system complexity while increasing the efficiency of system output [166]

Table 18 Disadvantages of PWM and MPPT

PWM	MPPT
PWM requires the solar input's nominal voltage to match the battery banks. [167]	The cost of MPPT controllers is higher [168]
No controller can handle 60 amps DC	The physical size of MPPT units is usually bigger [168]
PWM controllers have a finite amount of system expansion capacity [167]	Without MPPT controller manufacturer recommendations, sizing a suitable solar array might be difficult [168]
Cannot be utilized with 60A panels effectively [167]	MPPT controllers require, like photovoltaic modules in like strings in the solar array. [168]

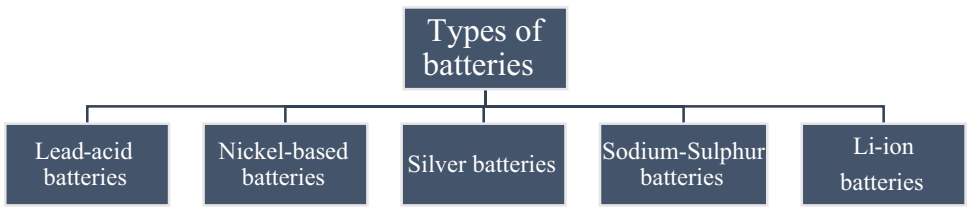

Fig. 19 Types of battery

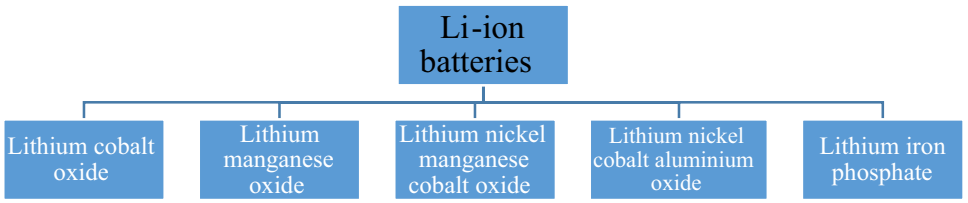

Fig. 20 Types of Li-ion battery

and ultra-capacitors are batteries used in electric vehicles (Fig. 19). Due to their high-density, high-power durability, longevity, and environmental friendliness, lithium-ion type batteries are suitable for Trinitor (Fig. 20) [170]. The advantages and disadvantages of batteries are displayed in Table 19 and Fig. 21a–d [171].

Thermo-electric generator

Thermo-Electric Generator is a device that generates electricity whenever, there is a temperature difference between the ends of a semiconductor. This principle is known as the Seebeck's Effect. The converse of it is also true, i.e., if electricity is flowing through a semiconductor, there will be temperature difference created. In this section, various types of materials for TEGs, their utility and applications are explored.

Thermo-electric generator

Vehicle waste detection employing TEGs has grown in popularity [176–178]. TEG converts thermal energy into electricity using Seebeck's effect and is compact and low-maintenance. Vehicle waste disposal methods like Organic Rankine or the turbocharger cycle are ineffective. TEGs don't have moving components or liquid like refrigerators,

Table 19 Advantages and disadvantages of different batteries

Battery type	Advantage	Disadvantage
VRLA	High specific power, Less cost, and efficiency [172]	Relatively heavy, low specific energy, small service life [172]
NI–CD	Deep charging and discharging without deterioration [173]	Low specific energy, recovery issue, and expensive [173]
NI-MH	Long lifespan, high specific energy, safety, and high temperature [174]	Memory effect, increased self-discharge, and expensive [173]
ZN-BR2	Less cost, Higher specific energy, and fast charging ability [174]	Temperature control required, Low specific power, and huge size [173]
ZN-CL2	Denser energy [174]	Less power and maintenance [173]
NA-S	Powerful, long-lasting, high energy density [174]	Expensive, unsafe, and temperature-related [174]
ZEBRA	High energy density, power, inexpensive, good undercharge and overcharge tolerance, and extended lifetime [174]	Self-discharge, low specific energy, temperature control [174]
LIAL-FES	High energy density and power, less weight and good undercharge and overcharge tolerance, longer lifetime [175]	Costly, require thermal management system [175]
LIAL-FES2	High energy density and power, less weight and good undercharge and overcharge tolerance, longer lifetime [175]	Costly, require thermal management system [175]
LI-polymer	High energy density and power, less weight and good undercharge and overcharge tolerance, longer lifetime [175]	Expensive, needs thermal management [175]
LI-ion	High specific power and energy density, reasonable efficiency, low weight and self-discharge, little memory effect, extended life [175]	Expensive, requiring heat control and overcharge/undercharge protection [175]

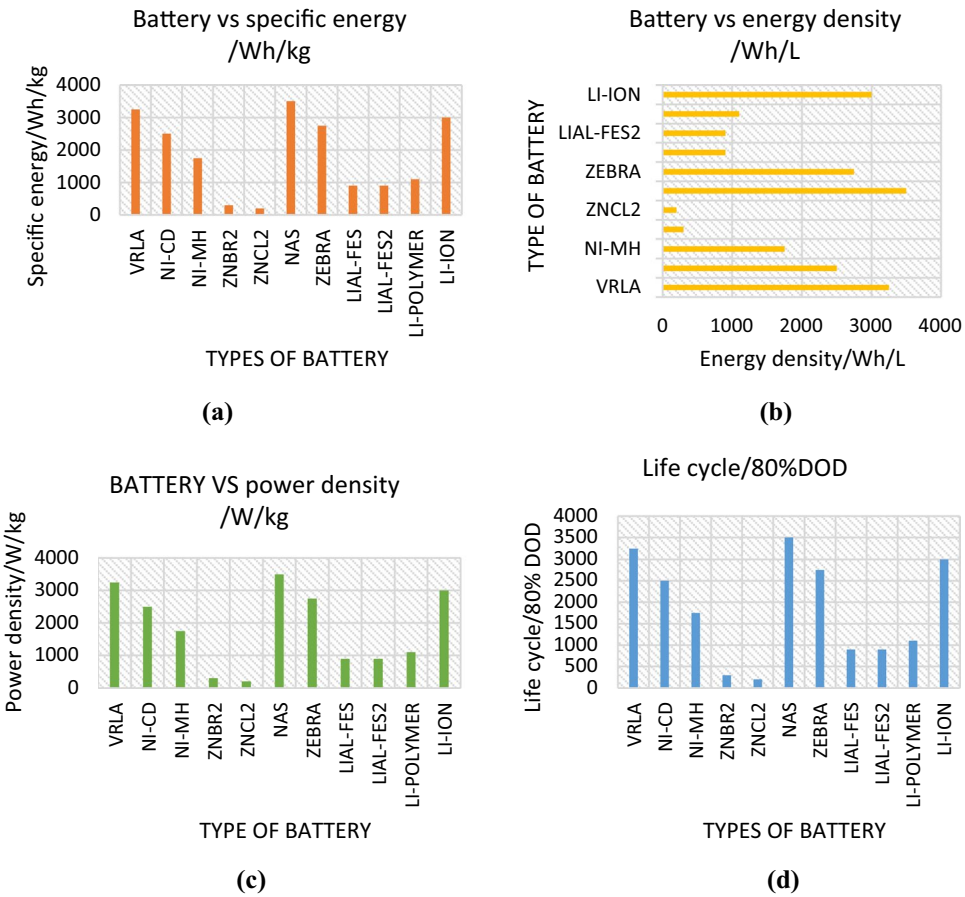

Fig. 21 **a** Battery versus specific energy **b** Battery versus energy density **c** Battery versus power density **d** Life cycle

Fig. 22 TEG materials

therefore they can handle this power with minimum vehicle performance disturbances.

Material researches of thermoelectric devices

Figure 22 shows the TEG material category.

Semiconductor Materials in Fig. 22 make TEG. Semiconductor materials (Seebeck coefficient above 100 V/°C) reduce thermal conductivity (k) without changing thermal diffusivity (α) on numerous objects, increasing Figure of Merit (ZT). Ilanga et al. examined and discussed organic *n*-type semiconductors for thermoelectric devices and concluded ZT is best for small bandgap semiconductors [179]. Some intermetallic compositions, including Mg_2X (X = Si, Ge, Sn) (ZT of Mg_2Si at 682 K = 0.86), have higher specifications like high coefficient of Seebeck, low electrical resistance, and low thermal performance. Anti-fluorite composition boosts performance and thermoelectricity [180]. Another strength is their anti-fluorite composition for high performance and effective thermoelectric properties.

Ceramic Metal oxides have better chemical stability, resistance to oxidation, low toxicity, and low cost than Te alloys, enabling longer-lasting electronics [181]. Ceramic, a thermoelectric material, can be used in combustion engines and incinerators for heat recovery [182]. Due to their low carrier mobility, they were not good TE materials before $Na_xCo_2O_4$ oxides. TE units with good TE characteristics have used cobalt oxide and cadmium oxide as *p*- and *n*-type semiconductors, respectively. Nonstoichiometric CdO has acceptable electrical conductivity. High valence elements and matching dopants reduced its resistivity [183]. Sb_2O_5 dopant on *n*-type SnO_2 increases electrical conductivity and has similar carrier mobility to oxide [184]. Wang et al. examined $Cd_{1-x}Pr_xO$ ceramic thermoelectric properties at higher temperatures. CdO doped with 0.1% Pr has 0.380 ZT at 1000 K [181, 185]. Zhu et al. examined TE performance after doping $CaMnO_3$ with lanthanides and other rare-earth elements [181]. The optimized dopant's ZT is 0.200 after replacing Yb or Dy. Double doping increases ZT substantially.

Polymer Toxic compounds, natural resource restrictions, and high-tech, expensive production methods limit inorganic thermoelectric materials [186]. The protective polymer matrix and conductive filler are safer and more ecologically friendly than previous thermoelectric modules for separating polymeric conductive compounds. Thus, mechanical flexibility, cheaper manufacture, solution process area, and lightweight were examined in these synthetic materials [187]. Elmoghani et al. shown that polymers can power thermoelectric machines with human body heat

Table 20 ZT of the Bi–Te-based material

Materials	Figures of merit	Temperature/K	References
Bi2Se0.5Te2.5	1.280	296	[191]
$(Bi,Sb)_2Te_3$	1.410	296	[192]
Bi2Te2.7Se0.3	1.270	296	[193]
Bi0.4Sb1.6Te3	1.260	296	[193]
P-type $(Bi,Sb)_2Te_3$ thermoelectric material	1.170	325	[194]
$Bi_2(Te,Se)_3$	1.010	296	[195]
P-type$(Bi_{0.26}Sb_{0.74})_2Te_3$ + 3%Te ingots	1.120	296	[196]
Bi–Sb–Te materials	1.150	352	[197]
(Bi2Te3)0.25(Sb2Te3)0.75	1.800	725	[198]
Bi2Te2.85Se0.15	2.380	775	[199]
Bi0.5Sb1.5Te3	1.930	695	[199]
Bi_2Te_3–Sb_2Te_3	1.260	422	[200]
95%Bi_2Te_3–5%Bi_2Se_3	1.670	725	[201]
90%Bi_2Te_3–5% Sb_2Te_3–5% Sb_2Se_3	1.770	695	[201]
$(Bi_2Se_3)_x(Bi_2Te_3)_{1-x}$	1.870	715	[202]
Bi_2Te_3	1.620	695	[202]
Bi2Te2.85Se0.15	1.860	695	[203]
p type Bi2Te3/Sb2Te3	2.40	302	[204]

[188]. Lu et al. examined ways to improve n-type polymers in thermoelectric devices [189]. Pang et al. examined the thermo-electric performance of a continuous polymer compound with CNTs and bismuth telluride, specifically a ZT-related value [190]. Table 20 shows that the most extensively utilized Bi-TE products are promising TE materials. This table indicates that ZT is closer to unity at room temperature, which is bad.

Application

The automobile sector has focused on thermoelectric generators, which transform outbound electricity in IC engines [189]. Fuel-efficient vehicles are used for gas extraction 40% and motor vehicles and equipment 25.5% [205]. Due to the wide variety of IC engines, different thermo-elements are needed to increase conversion efficiency. These applications utilize sub-thermoelectric materials due of their wide temperature range. Split TE materials include *N*- and *P*-type Bi_2Te_3 at low temperatures (250 °C), PTAGS and NPbTe at medium temperatures (250–500.0 °C), and Schuterite Materials ($PCeFe_3RuSb$) and ($NCoSb_3$) at higher temperatures (500–700 °C). The authors created a split material TE configuration to track segment thickness, thermal expansion coefficient, and module energy efficiency. This design uses flat TC solutions with a TE item between heat source and heat sink. Automotive applications use split TEGs and TEG cascades. This system's unique mechanical structure prevents partition instability. Willebrecht and Beatles Schmidt introduced two train car cascades in which Bi_2Te_3 (225 °C) and Mg_2SiSn / MnSi (415 °C) power the 2.55 kW cascade TEG [206]. IC engine manuals employ two TEG sites: radiator and exhaust heat exchanger. Crane et al. showed that TEG radiator integrated cooling system can absorb enough energy to power the alternator [162]. Ceramic substrates are suitable for Trinitor TEG to decrease heat transmission between TC arms and achieve substantial temperature differences between hot and cool surfaces.

Oxygen production

Oxygen production is done with the atmospheric air drawn in by the dehumidifier fan. Hot drying chamber exhaust is low temperature high moisturized air with moisture content of 60–70%. Water, a byproduct of PEM fuel cell, is sprayed over the flowing moist air stream making it highly humidified and saturated, which is dehumidified. The chilled air is combined with the moist air from TEG to enhance cooling effects. The collected water can be used as potable drinking water and excess is routed to an electrolyzer. An electrolyzer separates hydrogen and oxygen gases by passing electricity through water, later they are stored. The oxygen can be stored in separate gas balloons or pockets and used as an oxygenator for civilians when needed. When necessary, the H_2 and O_2 gases can be passed through the PEM fuel cell to produce electricity and water for the humidifier. After being stabilized and controlled by the charge controller, this electricity is stored in the battery.

PEM fuel cell

Proton Exchange Membrane Fuel cells are responsible for producing electricity using hydrogen and oxygen gases as intakes with water as by-product. The utility of this in the Trinitor is to generate power in vehicle using stored oxygen and hydrogen gas. In this section, the performance, application and working of PEMFC is discussed in detail.

PEM fuel cell

PEM fuel cells' adjustable design and low operating temperatures have made them popular as passenger vehicle and stationary power sources [207]. It generates electricity from fuel electrochemically like a battery [208]. The amount of fuel available for conversion to energy in a battery is limited, however with a PEM fuel cell, fuel is continually delivered into a system from an external source. One significant fuel cell type that can run at lower temperatures varying from −40 to 115 °C is polymeric membrane fuel cells [209].

Composition of proton-exchange membrane fuel cells

Figure 23 and Table 21 show PEM fuel cell components and specs. Table 22 displays the comparison of proton conductivity and PEMFC performance on Nafion-based composite membranes. Figure 24 shows the requirements to be fulfilled by PEM fuel cell for gasket.

Recently, poly-benzimidazole (PBI) membranes with a glass transition of 420 ℃ have shown promise for high-temperature functioning due to their thermal stability [231]. PBI and phosphoric acid-doped PBI (PA-PBI) membranes offer excellent proton conductivity, low gas permeability, low electro-osmotic drag, and excellent oxidative and thermal stability [232]. As PA doping and operation temperature

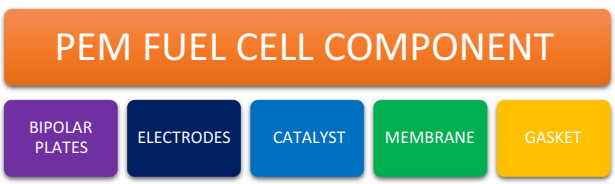

Fig. 23 Components in PEM fuel cell

Table 21 PEM component specifications

PEM component	Specifications
Bipolar plates	Bipolar plates made of graphite are the best for chemical resistance and conductivity [210] Internal cells of stack, if linked in series with the help of bimetallic plates increases the energy taken from fuel cell [211] For transport applications, PEMFCs should exhibit corrosion resistance (< 1.12 Acm^{-1}), electrical conductivity (> 99.99 Scm-1), and flexural strength (ASTM D789-10) (> 24.9 MPa). H2 transit rate (< 1.32_10–14($cm^3(cm^2s)^{-1}$)), area-specific resistance (0.01 W-cm^2), and weight (< 0.39 $KgKW^{-1}$) [212]
Electrodes	It includes carbon support, Pt patch, Nafion ionomer or Teflon binder [213]
Catalyst	Platinum (Pt) is a popular catalyst in PEMFC's because of its outstanding catalytic properties, operational stability and chemical stability Palladium is less expensive and abundant than Pt, has a strong catalytic effect, which reduces the overall cost of the fuel cell [214, 215]
Membrane	Perfluoro sulfonic acid (PFSA) polymer is the most frequently used membranes High temperature (100–190 °C) PEMFC are regarded as the future phase of fuel cells The advantages are: Faster electrochemical dynamics, Better and simplified water management, More efficient heat management and Better pollution tolerance Nafion-based coatings may be maintained at temperature below 130° C, the transition value of glass [216]. Table 18 shows the different types of Nafion based composite layers and their comparison to make it convenient for us to choose the best material for our system
Gasket	The problem of chemical deterioration of silicone rubber in PEM fuel cell [217] The gaskets are subjected to mechanical stress, acidic liquid solution, humid air Gasket polymers include polyacrylate rubber, fluorocarbon polymer, ethylene propylene rubber, nitrile rubber and its mixes, neoprene rubber, fluorosilicate rubber, butyl rubber, urethane rubber, and silicone rubber. Fig. 24 shows gasket needs

Table 22 Comparison of proton conductivity and PEMFC performance on Nafion-based composite membranes

Membranes	Conductivity or an activation energy	Temperature/°C	RH factor/%	PEMFC max. power density	Refs.
Nafion/12 mass%Phytic@MIL101	227.9 mS cm^{-1} and 15.16 kJ mol^{-1}	79.9	99.9	–	[218]
Nafion/10 mass% SAFHSS	99.99 mS cm^{-1}	99.9	99.9	–	[219]
Nafion/4 mass% GO	172 mS cm^{-1} and 13 kJ mol^{-1}	80.2	99.9	100 °C and RH = 26% and 214 mW cm	[220]
Nafion/0.05 mass%s-SWCNTs	15.7 mS cm^{-1}	99.9	99.9	65 °C and 649 mW cm	[220]
Nafion/5 mass% sPPSQ	159 mS cm^{-1}	122	99.9	–	[221]
Recast Nafion/20 mass% ZrSPP	49.9 mS cm^{-1}	112	98.0	100 °C and 700 mA cm @ 0.45 V *	[222]
Nafion/15 mass% Analcime	437.5 mS cm^{-1}	82	99.9	–	[223]
Nafion/1 mass% ZIF-8@GO	279 mS cm^{-1} and 13.4 kJ mol^{-1}	122	40.0	–	[224]
Nafion-0.6/UiO-66-NH_2 + UiO-66-SO_3H	258 mS cm^{-1}	89	95.0	–	[225]
Nafion-0.6/GO@UiO-66-NH_2	307 mS cm^{-1}	92	95.0	–	[225]
Nafion/3 mass% CPO-27(Mg)	13 mS cm^{-1}	50	99.0	50 °C and RH = 100% and 591 mW cm	[222]
Nafion/1 mass% SZM	2.98 mS cm^{-1}	81	35.0	80 °C and RH = 35% 550 mA cm @0.3 V	[226]
Nafion/1 mass% F-GO	17.5 mS cm^{-1}	72	20.0	70 °C and RH = 20% 300 mW cm	[227]
Nafion/3 mass% Fe_3O_4-SGO	11.7 mS cm^{-1} and 21.39 kJ mol^{-1}	119	20.0	120 °C and RH = 25% and 258.82 mW cm	[228]
Recast Nafion/14.3 mass% SiO_2-PWA	26.6 mS cm^{-1} and 11.4 kJ mol^{-1}	112	70.0	110 °C and RH = 70% 540 mA cm @0.4 V	[229]
meso-Nafion/19 mass% H3PW12O40	74 mS cm^{-1}	82	40.0	80 °C and RH = 50% 541 mW cm	[230]

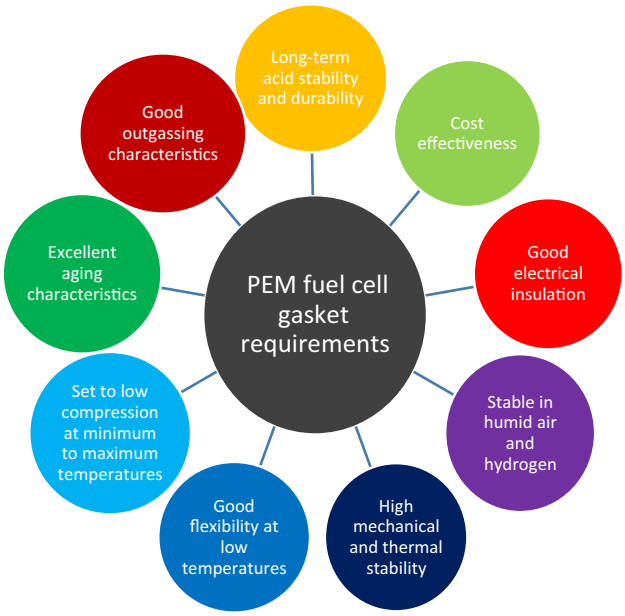

Fig. 24 PEMFC gasket requirements gasket

increase, mechanical stability decreases, whereas PBI molecular weight increases [233, 234].

Working process of pem fuel cells

Figure 25 shows the working process of PEMFC.

Application

Fuel cells are gaining popularity as pollution and carbon emissions decrease. PEMFCs are best for transportation. Wheelchairs, e-scooters, motorbikes, and wagons use proton-exchange membrane fuel cells [235], Fig. 26 lists a few uses.

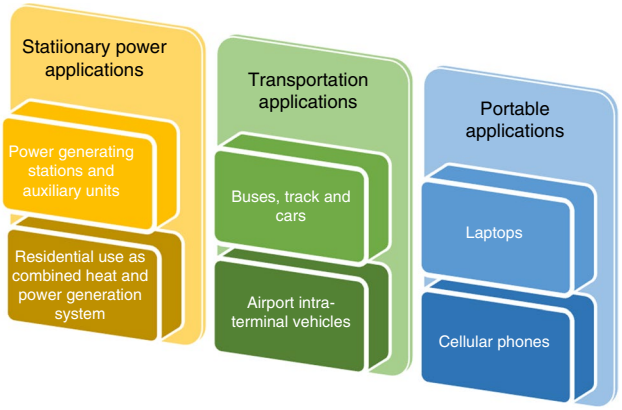

Fig. 26 Application of PEM fuel cell

Cold startup

Automobile fuel cells also need cold-start capability, as fuel cell vehicles must start in sub-zero conditions. When fuel cell temperatures drop below 0 °C, the fluid inside this electrode freezes and fills the vacuum space with ice. A hybrid battery may warm the stack above 0 °C to expel water by capillary action via liquid flow, making self-starting more practical, reliable, and attractive. A potential 10 s cold-start under 0.10 A cm from 30 °C requires a heat capacity to membrane area ratio of 300 J K^{-1}m [236].

Electrolyzer

An electrolyzer is a device responsible for breaking a water molecule into oxygen and hydrogen respectively. In our Trinitor, the purpose of an electrolyzer, is to generate oxygen for medical requirements. In this section, we discuss different types of electrolyzers, their performance and their utility in detail.

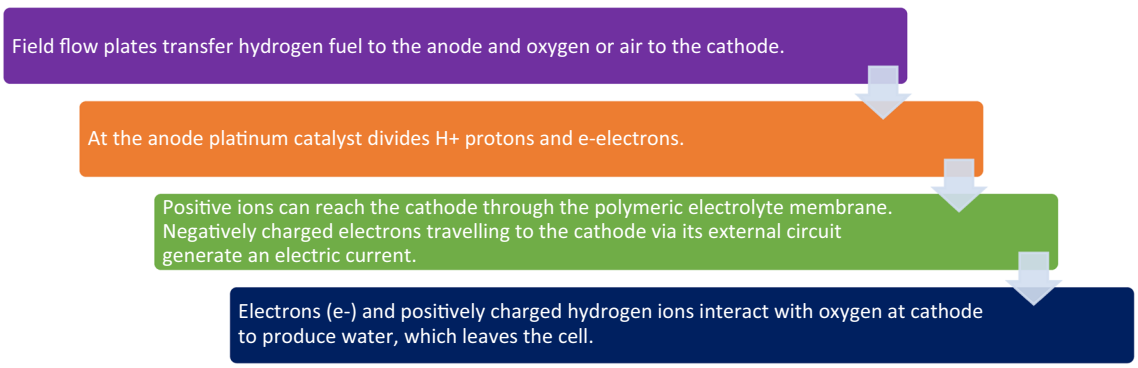

Fig. 25 PEMFC working process

Electrolyzer

Electrolyzers supply PEM fuel cell with H_2 and O_2. PVT modules/batteries power hydrogen electrolyzers. After compressing and storing H_2 in a gas tank, air is filtered and sent to the PEMFC stack to make O_2. Nonhomogeneous temperature changes may produce electrochemical response, reducing PEMFC lifetime, which is avoided by maintaining PEMFC working temperatures [237, 238]. A PVT module or battery generates electricity since the electrolyzer and fuel cell cannot consume and create power simultaneously (charge and discharge mode).

Types of electrolyzer

PEM, alkaline, and SOEC electrolyzers are the three primary types (Table 23). Electrolyzers work differently depending on the electrolyte. PEM Electrolyzer is ideal for Trinitor.

PEM electrolyzer

PEM electrolysis and PEM fuel cell technology use solid poly-sulfonated membranes (Nafion) as electrolytes [244]. Proton exchange membranes limit gas permeation, exhibit strong proton conductivity (0.10 ± 0.020 S cm^{-1}), low thickness (20.0–300 m), and rise under pressure [245]. PEM electrolyzers use electro catalysts like Pt/Pd for Hydrogen Evolution Reactions (HER) at the cathode and IrO2/RuO2 for Oxygen Evolution Reactions (OER) at the anode, making them more expensive than alkaline water electrolysis [245].

Components of electrolyzer

MEAs, current collectors, and separator plates make up a PEM electrolyzer. MEA splits the cell in half as the electrolyzer anode and cathode. IrO_2 powder was used to thermally treat the oxygen evolutionary anodic catalysis. Because of its high flux density (2.00 A cm), durability, proton conductivities, and mechanical strength, Nafion 115 membranes are used as solid polymer electrolytes [242]. Table 24 shows PEM fuel cells with varying cathode loadings. Current collectors are essential to the PEM electrolyzer's process and cell efficiency. Titanium plates are employed as potential current collectors in PEM electrolysis of water systems because to its electrical conductivity, structural robustness, and acid resistance. Bipolar plates and gaskets surround porous titanium plates that act as current collectors and gas diffusion layers (GDLs) on both sides of the

Table 23 Types of electrolyzer

Type of electrolyzer	Alkaline electrolyzer	PEM electrolyzer	SOEC (solid oxide) electrolyzer
Electrolytes	Aq. Potassium hydroxide (22–42 mass% KOH) [239]	Polymer membrane (e.g., Nafion) [239]	Yttria stabilized zirconia (ysz) Y2o3 + zro2[240]
Temperature/°C	20–80°c[241]	20–200°c[241]	650–1000°c[241]
Pressure/bar	< 30[241]	< 200[241]	< 25[241]
Energy Consumption kWh/Nm^3H_2	4.3–4.9[241]	3.6–4.0[241]	2.5–3.5[241]
Cathode	Ni or Ni–Mo alloys [239]	Pt or Pt–Pd [242]	Ni or YSZ [240]
Cathodic reaction	$2H_2O + 4e^- = 4OH^- + 2H_2$	$4H^+ + 4e^- = 2H_2$	$H_2O + 2e^- = O^{2-} + H_2$
Anode	Ni or Ni–Co alloys [239]	Ruo2 or iro2 [242]	LSM or YSZ [240]
Anodic reaction	$4OH^- = 2H_2O + O_2 + 4e^-$	$2H_2O = 4H^+ + O_2 + 4e^-$	$O^{2-} = 1/2\ O_2 + 2e^-$
Density of current/A cm^{-2}	0.20–0.40 [242]	0.60–2.0 [242]	0.30–2.0 [240]
Cell voltage/V	1.8–2.4 [242]	1.8–2.2 [242]	0.7–1.5 [240]
Voltage efficiency/%	62–82 [242]	67–82 [242]	Up to 100 [239]
Production rate/$m^3\ h^{-1}$	< 760 [239]	< 40 [239]	< 40 [239]
Advantages	Cost effective Long-term stability Mature technology Stack in the MW range [243]	Extremely high current densities High voltage efficiency High voltage efficiency Small system size High voltage efficiency [243]	Efficiency up to 100% Low energy demand Low capital cost. [243]
Dis-advantages	Inadequate current densities Purity degree Low partial load, low dynamics [243]	High prices of the components, Corrosive environment, Low durability[243]	Mechanically unstable Laboratory stage Durability (brittle ceramics) Bulky system design Safety issue[243]
Challenges	Increased durability/reliability Oxygen/air evolution [241, 243]	Improvement of electrolyte Reduction of noble-metal utilizations [243]	C deposition, Microstructural changes in the electrodes[243]

Table 24 Summary of full PEM Electrolyzer with a cathode

Cathode (Loading in mg cm)	Membrane	Anode/mg cm	Temperature/°C	Performance	Stability	Refs.
MoS_2	Nafion 117	Iridium oxide	80.0	0.020 A cm at 1.90 V	–	[248]
47 mass% MoS_2/CB (2.5)	Nafion 117	Iridium oxide	80.0	0.30 A cm at 1.90 V	Increasing current density after 18 h	[248]
MoS_2/rGO	Nafion 117	Iridium oxide	80.0	0.10 A cm at 1.90 V	–	[248]
MoS_x/CB	Nafion 115	Ir black	80.0	0.90 A cm at 2.1 V	Stable current density over 24 h	[249]
Mo_3S_{13}/CB	Nafion 115	Ir black	80.0	1.1 A cm at 2.1 V	current density decreased by more than 100 mA/cm^2 after 24 h	[249]
MoS_2 nCapsules	Nafion 117	Iridium oxide	80.0	0.06 A cm at 2.1 V	Stable current density for 200 h	[250]
MoS_x/C-cloth	Nafion 117	Ruthenium (IV) oxide	80.0	0.3 A cm at 2.1 V	–	[251]
MoS_x/C-paper	Nafion 212	Iridium oxide	90.0	0.35 A cm at 1.9 V	Stable current density over 4 h	[252]
Pyrite FeS_2	Nafion 115	Iridium oxide	80.0	1.0 A cm at 2.10 V	Stable for 100 h	[253]
Greigite Fe_3S_4	Nafion 115	Iridium oxide	80.0	1.0 A cm at 2.13 V	Stable for 100 h	[253]
Pyrrholite Fe_9S_{10}	Nafion 115	Iridium oxide	80.0	1.0 A/cm^2 at 2.16 V	Stable for 100 h	[253]
30.00 mass% Pd/P-doped C (carbon black)	Nafion 115	Ruthenium (IV) oxide	80.0	1.0 A cm at 2 V	Stable for 500 h	[254]
30.00 mass% Pd/N-doped CNTs	Nafion 115	Ruthenium (IV) oxide	80.0	1.0 A cm at 2.01 V	Stable for 50 h	[255]
30.00 mass% Pd/P-doped Graphene	Nafion 115	Ruthenium (IV) oxide	80.0	1.0 A cm at 1.96 V	Cell voltage increased to 2.0 V after 2000 h	[256]
Activated single-wall carbon nanotubes	Nafion 115	$Ir_{0.7}Ru_{0.3}Ox$	80.0	1.0 A cm at 1.65 V	Stable for 90 h	[257]

MEA. Current collectors allowed electrical current to flow between the electrode and bipolar plates [246]. Titanium grid systems, carbon current collectors, and stainless-steel grids have inferior electrochemical characteristics than pure titanium plates. PEM electrolyzer separator plates are currently stainless steel, titanium, and graphite. Many electrolyzer systems use different separator plate designs to improve performance, but a horizontal straight flow field has shown promising electrochemical activity, particularly in PEM electrolyzers [247].

Challenges of electrolyzer

Thermally generated IrO_x has higher stability but lesser activity than electrochemically manufactured oxides or hydrous IrO_x. A rising number of experiments on relatively long electrolysis operations lasting hundreds or even thousands of hours have already been published in the recent literature. At a reduced current load of 1.0 A cm^2, IrO_x sustained on a Ti catalyst containing 50% Ir and then a low catalyst concentration of 0.125 cm^2 operated for more than 1 thousand hours [258]. The highest reported stability was achieved with nano—structured thin film (NSTF) cell, that attained 5 thousand hours with the same current load of 2.0 A cm^2 and an Ir loading of 0.255 mg cm^2 [259]. No other supporting catalyst has achieved the same level of catalytic durability as titanium-assisted catalyst [260].

Application of electrolyzer

The PEM electrolyzer is a low-carbon energy and chemical storage solution for enterprises. Hydrogen is an attractive storage device for surplus sustainable power because it can be used for energy production during peak demand periods, oil and gas grid supplementation for efficiency improvements, transportation fueling, and chemical biofuel production for green fertilizer and other chemicals. [261]. The Polymer Electrolyte Membrane (PEM) Electrolyzer, excellent for large-scale hydrogen generation, uses an ionically conductive solid polymer. [262].

Analysis of trinitor

Advantages and limitations of each technique

Electricity generation

Turbo-compounding provides numerous advantages. It enables the recovery of waste heat from engine exhaust, leading to a reduction in CO_2 emissions and enhanced fuel efficiency. Approximately 30% of exhaust gas can be recycled as a power source, thereby improving overall efficiency [263]. Moreover, turbo-compounding has the potential to boost engine mechanical power, with research indicating an increase of up to 18% in power output. It can also generate additional electrical power from engine exhaust energy, with potential gains of up to 1.1 kW. In summary, turbo-compounding presents opportunities for enhanced performance, lowered emissions, and increased fuel efficiency in internal combustion engines. Turbo-compounding does have its limitations, particularly in terms of power losses and increased pumping work. The power turbine, which is situated in series with the main turbine, experiences power losses due to higher back pressure, leading to increased pumping losses [264]. Furthermore, in turbo-compounding setups within passenger cars, the utilization of waste heat is limited since only a small portion of the exhaust energy is required for compressing the intake air.

MPPT charge controllers provide various advantages within PVT systems. They excel at extracting more electricity from solar panels by operating at the panel's maximum power voltage, resulting in improved charging efficiency and increased power output. These controllers effectively manage battery charging, ensuring it's done correctly and preventing overcharging. MPPT controllers outperform PWM controllers, boasting higher efficiency levels ranging from 94 to 99% [265]. Overall, the incorporation of MPPT charge controllers in PVT systems enhances battery charging regulation, boosts efficiency, and maximizes power extraction from solar panels. However, it's essential to note that unchecked energy consumption by electrical equipment can lead to system failures and a reduced system lifespan when using MPPT charge controllers [266].

Drying of produce

Both hot air and infrared food drying methods offer several advantages. Infrared radiation, when applied carefully, can enhance drying kinetics, resulting in faster drying at elevated temperatures and reduced distances. However, it is crucial to avoid extreme values to prevent overheating. The utilization of infrared radiation can also enhance food quality by lowering water activity, minimizing color changes, and retaining essential nutrients. In numerous studies, infrared drying has proven to be more efficient and capable of producing higher-quality products compared to conventional drying techniques. Furthermore, the combination of hot air and infrared heating can deliver uniform heating, reduce drying duration, and enhance energy efficiency [267]. In a hot air-infrared system, maintaining a minimum hot air velocity of 0.3 m/s is advisable to ensure proper control of product quality. Overall, both hot air and infrared drying methods have their respective advantages and disadvantages, and the choice should be based on the specific requirements of the drying process [268].

Space cooling/heating

The advantages of Peltier and Seebeck effect cooling/heating systems encompass their utilization of green infrastructure, absence of harmful gases, straightforward design and construction, compact dimensions, and eco-friendliness. These systems do not rely on moving components like compressors or solution pumps, reducing the risk of mechanical failures. Moreover, they have the potential to mitigate the adverse impacts associated with traditional refrigeration systems, including issues such as skin cancer, ozone depletion, and contributions to global warming. Additionally, cooling/heating modules based on the Peltier effect can be fine-tuned for optimal coefficient of performance and cooling/heating capacity, thus enhancing their overall efficiency. Notably, Peltier effect cooling systems have been effectively deployed in various applications, such as air conditioning and emergency cooling for electric vehicle batteries, ensuring user safety and comfort. Nonetheless, Peltier effect cooling does have limitations, including relatively modest cooling performance when compared to conventional refrigeration. Another constraint involves the necessity to optimize the power supply current to achieve the desired cooling/heating capacity and coefficient of performance [269].

Oxygen generation

The utilization of PEM electrolyzers for oxygen generation offers several advantages. Firstly, it enables highly efficient electrodes that are straightforward to manufacture and cost-effective. Secondly, PEM electrolyzers are adaptable and can function with both vapor and liquid feed systems, providing versatility for various applications. Moreover, these electrolyzers play a crucial role in the production of renewable hydrogen, which is essential for achieving decarbonization and sustainability goals [270]. However, the commercialization of low-temperature fuel cells and electrolyzers faces

challenges related to stability. Addressing these challenges necessitates the exploration of novel approaches for assessing degradation. Factors such as electrode architecture, the nature of the electrolyte, reactant and product transport, and operating conditions should all be considered in this context [271].

Overall performance

The polygenerative process typically provides greater efficiency compared to the individual efficiencies of the processes it involves. Polygenerative systems often involve synergistic interactions between processes, where the output of one process complements or enhances the performance of another. This cooperation between processes can lead to higher overall efficiency than if they were operated independently. Thus, theoretically with literature support trinitor can achieve overall efficiency of 40.12–54.81%. The actual improvement in efficiency may vary slightly depending on the system's design and components; nonetheless, the underlying thermodynamic concepts support the theoretically achieved efficiency range with literature support. An article with empirical results from real-time applications and case studies will be published soon. When temperatures exceed 600 °C, the Trinitor excels in capturing waste heat, recovering nearly 40–45% of the energy from exhaust gases [272]. This highlights its effectiveness in capturing energy that would have otherwise been squandered, helping to promote more sustainable energy use [273]. Trinitor dramatically reduces exhaust gas emissions while an engine runs at a lower load. This decrease is crucial since it coincides with a motor's peak efficiency and emphasizes the Trinitor's reduction in emission's beneficial effects on the environment [274]. Table 25 lists the performance of individual components used in Trinitor reported in other articles.

Conclusions

A comprehensive review of all the techniques, principles, chemicals, components, etc. available for exhaust waste heat recovery forms the basis of this paper's investigation into, and selection of, the necessary components for the proposed sustainable conceptual polygenerative system model "Trinitor" for diesel vehicles. According to the findings of the review:

- The use of SiC wall flow-Diesel Particulate Filters (DPF), a paraffin-based Latent Heat Storage (LHS) System, and electric-assisted turbo compounding allows the electricity production unit to operate efficiently at minimal cost.
- The produce drying unit can work efficiently and cheaply by using hot air drying or infrared drying, a revolving wicks humidifier, and a cooling coil type dehumidifier.
- The space cooling/heating unit requires water type PV/T collector, Maximum Power Point Tracking (MPPT) charge controller, Lithium-ion batteries and ceramic-based TEGs for efficient output.
- A (Proton Exchange Membrane) PEM electrolyzer with appropriate components (bipolar plates, electrodes, catalyst, membrane, and gasket) contributes to the efficient operation of the oxygen production unit.

Future scope

- A future publication will present an energy, exergy, economic, and environmental analysis of the Trinitor prototype, constructed using the components identified in this review.

Table 25 Performance of individual components reported in other articles

Components	Power output	Efficiency/%	Hydrogen rate	Oxygen rate	Energy density	Air Drying rate	Water flow rate	References
Diesel engine	110–294 KW (150–400 HP)	35–45	–	–	32–36 MJ kg^{-1}	–	–	[275]
Generator	960 W	50–70	–	–	–	–	–	[276]
Hot air dryer	800 W	60–90	–	–	–	2 m s^{-1}	–	[277, 278]
Humidifier	100 W	–	–	–	–	–	–	[279]
Dehumidifier	300–800 W	–	–	–	–	–	–	[280]
PVT panel	100–400 W/m^2	50–80	–	–	–	–	0.083 kg/sec	[281, 282]
Charge Controller	It doesn't produce power	90–98	–	–	–	–	–	[283]
Battery	1.2 kWh	70–90	–	–	150–250 Wh kg^{-1}	–	–	[284]
TEG	37 W	5–10	–	–	0.5–1 Wh cm^2	–	–	[285]
PEM Fuel cell	5 kW–1 MW	30–40	0.07 L min^{-1}	0.04 L min^{-1}	39.7 kW kg^{-1}	–	–	[286, 287]
Electrolyser	5 kW–2 MW	60–80	36.26 kg/h	287.74 kg/h	–	–	–	[288, 289]

- The challenges that could arise during the implementation of Trinitor, along with their respective solutions, have been presented:
- When moving critical parts and equipment to difficult locations, logistical issues may occur. When building successful transit and setup solutions, we must consider transportation methods, assembly requirements, and on-site help. Selecting the optimal locations for storing important parts near the deployment area allows for faster assembly. This saves time on transportation [290].
- On a big scale in remote locations, the Trinitor setup may lack the necessary supporting infrastructure. Thoroughly analyze the location and collaborate with local officials to ensure that appropriate infrastructure is available or can be created. Simplifying shipping and on-site assembly, use modular designs and smart logistics planning can be done to overcome the challenge [291].
- The cost of implementing a large-scale Trinitor system in certain locations can be a significant barrier. To address this, consider exploring funding options, grants, or partnerships that can help offset costs and make the technology economically viable for deployment in remote areas [32].
- Ensure that the supplies and equipment required for a substantial Trinitor installation are readily accessible or can be obtained in a sustainable manner. Exploring alternative materials and implementing efficient resource management techniques can help reduce costs and optimize resource utilization [292, 293].
- Ensuring a reliable hot gas or air source in remote or hard-to-access areas can be a challenge. To reduce dependence on a single energy source, it is essential to conduct a thorough analysis of the location's solar radiation patterns and explore potential alternative energy sources. One solution is to implement hybrid energy systems that combine solar, biomass, or other renewable energy sources to ensure a consistent energy supply [294].
- Even though, the proposed application for this process is focused on mobility and small-scale heavy-duty vehicles specifically, this process can also be applied on a large scale and a stationary plant-like setup can be done in very inaccessible locations to satisfy basic power, water needs and temperature modulation of products. When scaling up the Trinitor process for larger stationary plant-like configurations, there may be challenges in maintaining efficiency and optimal performance. To address this, rigorous engineering and modeling studies should be conducted to optimize the system design. Consider factors such as heat distribution, material constraints, and the seamless integration of components to ensure sustained performance [295].
- Maintaining consistent and reliable performance of the Trinitor system, particularly in fluctuating environmental conditions, poses a significant challenge. To address this, conduct simulations and tests should be in diverse environments to ensure the system's dependability and resilience. Redundancy techniques and fail-safes should be implemented to prevent performance interruptions and ensure continuous energy production [296, 297].
- The development and adoption of Trinitor technology may be hampered by complex and ever-changing regulatory frameworks related to renewable energy. Participating in policy advocacy and collaborating with government agencies to assist create favorable policies that promote the usage of renewable energy. Collaborating with legal specialists to streamline the Trinitor deployment approval process and ensure compliance with current legislation. Joining trade associations to influence policy debates and establish rules that will benefit your industry will help overcome regulatory challenges [298].

Feasibility and practicality

This section discusses the viability and practicability of introducing the Trinitor system, with a particular emphasis on cost-effectiveness, maintenance requirements, widespread acceptance, and compatibility with existing vehicle systems.

- As per a research report evaluation, the initial installation of a Trinitor system in automobiles can incur substantial costs. This technology may prove prohibitively expensive for certain applications, particularly when considering the high cost of system components and vehicle integration. However, as a polygenerative system, Trinitor effectively minimizes expenses associated with multiple outputs. Consequently, it can achieve a swift payback period and a prolonged operational lifespan, ultimately resulting in cost-effective operations for the majority of its lifecycle. The recommended approach for cost effectiveness involves exploring government subsidies, tax rebates, or incentives to offset initial expenses. Enhancing the efficiency of the supply chain and collaborating with dependable and economical suppliers can lower material and logistical costs, ultimately enhancing overall cost-effectiveness. Negotiating advantageous contracts and simplifying procurement procedures are crucial components. Furthermore, continuous research and development efforts to reduce manufacturing costs of Trinitor components and enhance productivity can further contribute to increased cost-effectiveness [299].
- Maintenance of a polygenerative system used for waste heat recovery is essential to ensure that it continues

to provide energy savings and environmental benefits. Due to the limited number of moving components in the Trinitor system, its maintenance requirements are minimal. Implementing fundamental maintenance procedures, including routine inspections, cleaning, sensor calibration, performance monitoring, energy audits, optimization, adherence to safety protocols, maintaining a spare parts inventory, and ensuring environmental compliance, is essential for prolonging the system's longevity. However, specialized maintenance and a workforce with the necessary expertise can potentially facilitate broader adoption. The Trinitor system, whether applied in a power plant or as part of a vehicle, requires regular maintenance to ensure peak performance. Overcoming the maintenance challenge requires the development of user-friendly maintenance protocols and training programs, including digital training methods. Collaboration with local service providers or offering incentives for training can help guarantee the availability of a skilled workforce for system maintenance. Constructing the Trinitor system to withstand extreme environmental conditions and utilizing high-quality, durable materials can effectively minimize maintenance needs and extend the system's operational lifespan. Enhanced durability results in reduced frequency of replacements and repairs, leading to cost savings and improved overall performance [14].

- The integration of Trinitor systems may pose mainly space, compatibility, mass and balance challenges, especially with older vehicles. Adapting the Trinitor model to operate effectively across different car makes and models can be a complex task. To address this, designing new vehicle models in collaboration with automobile manufacturers, which feature integrated Trinitor systems, will ensure compatibility and optimal performance. Additionally, to promote wider adoption, exploring retrofitting options for older vehicles should be considered [6].
- Enhancing the adoption of Trinitor technology may require bolstering its credibility. The public might require assistance in understanding the benefits of this technology or may have concerns regarding its efficiency and safety. To mitigate these concerns, public awareness campaigns, educational programs, and the presentation of successful case studies can play a pivotal role. Collaborating with educational institutions and media for informative campaigns can positively influence public acceptance. Additionally, real-world examples of vehicles on the road utilizing Trinitor technology can significantly bolster public confidence in its capabilities and safety.

Acknowledgements The authors extend their appreciation to the Deanship of Scientific Research at King Khalid University for funding this work through large group Research Project under grant number RGP 1/80/44. The researchers would like to acknowledge Deanship of Scientific Research, Taif University, for funding this work.

Funding Open access funding provided by the Scientific and Technological Research Council of Türkiye (TÜBİTAK).

References

1. Ghasemian S, Faridzad A, Abbaszadeh P, Taklif A, Ghasemi A, Hafezi R. An overview of global energy scenarios by 2040: identifying the driving forces using cross-impact analysis method. Int J Environ Sci Technol. 2020. https://doi.org/10.1007/s13762-020-02738-5.
2. Larsson M. Global energy transformation: Four necessary steps to make clean energy the next success story. London: Palgrave Macmillan; 2009.
3. Samaras C, Nuttall WJ, Bazilian M. Energy and the military: convergence of security, economic, and environmental decision-making. Energ Strat Rev. 2019;26:100409. https://doi.org/10.1016/j.esr.2019.100409.
4. Wang KH, Su CW, Lobonţ OR, Umar M. Whether crude oil dependence and CO_2 emissions influence military expenditure in net oil importing countries? Energy Policy. 2021;153:112281. https://doi.org/10.1016/J.ENPOL.2021.112281.
5. IRENA (2021), World Energy Transitions Outlook: 1.5°C Pathway, International Renewable EnergyAgency, Abu Dhabi.
6. Mobin SA, Saif SA, Najim SN, Umar Farooq PO, Farhan PA (2017) Utilization of exhaust gas of vehicle for electricity generation. Available: www.irjet.net
7. He M, Wang E, Zhang Y, Zhang W, Zhang F, Zhao C. Performance analysis of a multilayer thermoelectric generator for exhaust heat recovery of a heavy-duty diesel engine. Appl Energy. 2020;274:115298. https://doi.org/10.1016/J.APENERGY.2020.115298.
8. Deng YD, Hu T, Su CQ, Yuan XH. Fuel economy improvement by utilizing thermoelectric generator in heavy-duty vehicle. J Electron Mater. 2017;46(5):3227–34. https://doi.org/10.1007/S11664-016-4996-1/METRICS.
9. Bjørk R, Sarhadi A, Pryds N, Lindeburg N, Viereck P. A thermoelectric power generating heat exchanger: part I–Experimental realization. Energy Convers Manag. 2016;119:473–80. https://doi.org/10.1016/j.enconman.2016.04.042.
10. Teng H, Regner G (2009) Improving fuel economy for hd diesel engines with WHR rankine cycle driven by EGR cooler heat rejection. https://doi.org/10.4271/2009-01-2913
11. Cipollone R, Di Battista D, Bettoja F. Performances of an ORC power unit for waste heat recovery on heavy duty engine. Energy

Procedia. 2017;129:770–7. https://doi.org/10.1016/j.egypro.2017.09.132.
12. A study on the use of a stirling engine generator to reduce fuel oil consumption onboard a tanker ship. Accessed on Oct 15, 2023. Available: https://medwelljournals.com/abstract/?doi=jeasci.2016.2044.2049
13. Douadi O, Ravi R, Faqir M, Essadiqi E. A conceptual framework for waste heat recovery from compression ignition engines: technologies, working fluids & heat exchangers. Energy Convers Manag: X. 2022;16:100309. https://doi.org/10.1016/J.ECMX.2022.100309.
14. Jouhara H, Khordehgah N, Almahmoud S, Delpech B, Chauhan A, Tassou SA. Waste heat recovery technologies and applications. Therm Sci Eng Prog. 2018;6:268–89. https://doi.org/10.1016/j.tsep.2018.04.017.
15. Kim S, Park S, Kim S, Rhi SH. A thermoelectric generator using engine coolant for light-duty internal combustion Engine-Powered Vehicles. J Electron Mater. 2011;40(5):812–6. https://doi.org/10.1007/S11664-011-1580-6/METRICS.
16. Muralidhar N, Himabindu M, Ravikrishna RV. Modeling of a hybrid electric heavy duty vehicle to assess energy recovery using a thermoelectric generator. Energy. 2018;148:1046–59. https://doi.org/10.1016/J.ENERGY.2018.02.023.
17. Teng H, Klaver J, Park T, Hunter GL, Van Der Velde B, (2011) A rankine cycle system for recovering waste heat from hd diesel engines—WHR system development, SAE 2011 world congress and exhibition, https://doi.org/10.4271/2011-01-0311
18. Bettoja F, Perosino A, Lemort V, Guillaume L, Reiche T, Wagner T. NoWaste: waste heat re-use for greener truck. Transp Res Procedia. 2016;14:2734–43. https://doi.org/10.1016/j.trpro.2016.05.456.
19. Venkatesh J, Kumar K, Kavin R. Generating electricity by using exhaust gas. Int J Eng Sci Comput. 2018;8(4):16905–7.
20. Zohuri B, McDaniel P. Thermodynamics in nuclear power plant systems, Second edition. Thermodyn Nucl Power Plant Syst. 2018. https://doi.org/10.1007/978-3-319-93919-3/COVER.
21. Patil DS, Arakerimath RR, Walke PV. Thermoelectric materials and heat exchangers for power generation—a review. Renew Sustain Energy Rev. 2018;95:1–22. https://doi.org/10.1016/j.rser.2018.07.003.
22. Kramer DM, Parker GG. Current state of military hybrid vehicle development. Int J Electr Hybrid Veh. 2011;3(4):369–87. https://doi.org/10.1504/IJEHV.2011.044373.
23. Rizzo DM, (2014) Digital Commons @ Michigan Tech military vehicle optimization and control
24. Li J, et al. Toward low-cost, high-energy density, and high-power density lithium-ion batteries. Jom. 2017;69(9):1484–96. https://doi.org/10.1007/s11837-017-2404-9.
25. Santucci A, Sorniotti A, Lekakou C. Power split strategies for hybrid energy storage systems for vehicular applications. J Power Sour. 2014;258:395–407. https://doi.org/10.1016/j.jpowsour.2014.01.118.
26. Mężyk P, Przybyła G, Petela K. Analysis of thermal parameters of heat storages for use in vehicles with combustion engines. Combust Engines. 2019;179(4):119–25. https://doi.org/10.19206/ce-2019-419.
27. Brzeżański M, Mężyk P. Heat balance of the military vehicle. Combust Engines. 2017;170(3):131–4. https://doi.org/10.19206/ce2017-322.
28. Dinker A, Agarwal M, Agarwal GD. Heat storage materials, geometry and applications: a review. J Energy Inst. 2017;90(1):1–11. https://doi.org/10.1016/j.joei.2015.10.002.
29. Conklin JC, Szybist JP. A highly efficient six-stroke internal combustion engine cycle with water injection for in-cylinder exhaust heat recovery. Energy. 2010;35(4):1658–64. https://doi.org/10.1016/J.ENERGY.2009.12.012.
30. Wang T, Zhang Y, Peng Z, Shu G. A review of researches on thermal exhaust heat recovery with Rankine cycle. Renew Sustain Energy Rev. 2011;15(6):2862–71. https://doi.org/10.1016/J.RSER.2011.03.015.
31. Edwards KD, Wagner R, Briggs T. Investigating potential light-duty efficiency improvements through simulation of turbo-compounding and waste-heat recovery systems. SAE Tech Papers. 2010. https://doi.org/10.4271/2010-01-2209.
32. Shu G, Liang Y, Wei H, Tian H, Zhao J, Liu L. A review of waste heat recovery on two-stroke IC engine aboard ships. Renew Sustain Energy Rev. 2013;19:385–401. https://doi.org/10.1016/J.RSER.2012.11.034.
33. Gülmez Y, Özmen G. Effect of exhaust backpressure on performance of a diesel engine: neural network based sensitivity analysis. Int J Automot Technol. 2022;23(1):215–23. https://doi.org/10.1007/S12239-022-0018-X/METRICS.
34. Callahan TJ, Branyon DP, Forster AC, Ross MG, Simpson DJ. Effectiveness of mechanical turbo compounding in a modern heavy-duty diesel engine. Int J Automot Eng. 2012;3(2):69–73.
35. Sjöberg M, Vuilleumier D, Yokoo N, Nakata K (2017) Effects of gasoline composition and octane sensitivity on the response of DISI engine knock to variations of fuel-air equivalence ratio, COMODIA 2017. In: 9th international conference on modeling and diagnostics for advanved engine systems, https://doi.org/10.1299/JMSESDM.2017.9.B307.
36. Khair MK. A review of diesel particulate filter technologies. SAE Tech Papers. 2003. https://doi.org/10.4271/2003-01-2303.
37. Khair MK (2003) A review of diesel particulate filter technologies, SAE Technical Papers, 724. https://doi.org/10.4271/2003-01-2303
38. Kočí P, et al. 3D reconstruction and pore-scale modeling of coated catalytic filters for automotive exhaust gas aftertreatment. Catal Today. 2019;320:165–74. https://doi.org/10.1016/J.CATTOD.2017.12.025.
39. Seo JM, Park WS, Lee MJ. The best choice of gasoline/diesel particulate filter to meet future particulate matter regulation. SAE Tech Papers. 2012. https://doi.org/10.4271/2012-01-1255.
40. Guan B, Zhan R, Lin H, Huang Z. Review of the state-of-the-art of exhaust particulate filter technology in internal combustion engines. J Environ Manage. 2015;154:225–58. https://doi.org/10.1016/J.JENVMAN.2015.02.027.
41. Yildiz I, Caliskan H, Mori K. Effects of cordierite particulate filters on diesel engine exhaust emissions in terms of pollution prevention approaches for better environmental management. J Environ Manage. 2021;293:112873. https://doi.org/10.1016/J.JENVMAN.2021.112873.
42. Se K, Baines N (2014) ASME GT2010, pp 1–5
43. N. Corporation, NoTox silicon carbide diesel particulate wall flow filter. Technical Product Information Series, (ProSpec4) 4. Edition, September 1995. ISBN 87-985237-3-2
44. Brillant S, Zikoridse G. Metal fibre diesel particulate filter : function and technology. SAE Tech Papers. 2005. https://doi.org/10.4271/2005-01-0580.
45. Brillant S (2005) Metal fibre diesel particulate filter, 724
46. Kenisarin M, Mahkamov K. Solar energy storage using phase change materials. Renew Sustain Energy Rev. 2007;11(9):1913–65. https://doi.org/10.1016/J.RSER.2006.05.005.
47. Fernandes D, Pitié F, Cáceres G, Baeyens J. Thermal energy storage: How previous findings determine current research priorities. Energy. 2012;39(1):246–57. https://doi.org/10.1016/J.ENERGY.2012.01.024.

48. Fatih Demirbas M. Thermal energy storage and phase change materials: an overview. Energy Sour Part B: Econ Plan Policy. 2006;1(1):85–95.
49. Rathod MK, Banerjee J. Thermal stability of phase change materials used in latent heat energy storage systems: a review. Renew Sustain Energy Rev. 2013;18:246–58. https://doi.org/10.1016/J.RSER.2012.10.022.
50. Zhang Y, Zhou G, Lin K, Zhang Q, Di H. Application of latent heat thermal energy storage in buildings: state-of-the-art and outlook. Build Environ. 2007;42(6):2197–209. https://doi.org/10.1016/J.BUILDENV.2006.07.023.
51. Pilkington Solar International GmbH, Survey of thermal storage for parabolic trough power plants period of performance: September 13, 1999 June 12, 2000: survey of thermal storage for parabolic trough power plants period of performance, Nrel, p 61, 2000
52. Paris J, Falardeau M, Villeneuve C. Thermal storage by latent heat: a viable option for energy conservation in buildings. Energy Sour. 1993;15(1):85–93. https://doi.org/10.1080/00908319308909014.
53. Shukla A, Buddhi D, Sawhney RL. Thermal cycling test of few selected inorganic and organic phase change materials. Renew Energy. 2008;33(12):2606–14. https://doi.org/10.1016/j.renene.2008.02.026.
54. Ootake M, et al. Development of diesel engine system with DPF for the european market. SAE Tech Papers. 2007. https://doi.org/10.4271/2007-01-1061.
55. Bo H, Gustafsson EM, Setterwall F. Tetradecane and hexadecane binary mixtures as phase change materials (PCMs) for cool storage in district cooling systems. Energy. 1999;24(12):1015–28. https://doi.org/10.1016/S0360-5442(99)00055-9.
56. Bromberg L, Cohn DR, Wong V (2005) Regeneration of diesel particulate filters with hydrogen rich gas* MIT plasma science and fusion center
57. Southward BWL, Basso S, Pfeifer M. On the development of low PGM content direct soot combustion catalysts for diesel particulate filters. SAE Tech Papers. 2010. https://doi.org/10.4271/2010-01-0558.
58. Babich MW, Hwang SW, Mounts RD. The search for novel energy storage materials using differential scanning calorimetry. Thermochim Acta. 1992;210:83–8. https://doi.org/10.1016/0040-6031(92)80279-6.
59. Babich MW, Benrashid R, Mounts RD. DSC studies of new energy storage materials. Part 3. Thermal and flammability studies. Thermochim Acta. 1994;243(2):193–200. https://doi.org/10.1016/0040-6031(94)85054-2.
60. Pielichowski K, Flejtuch K, Pielichowski J. Step-scan alternating DSC study of melting and crystallisation in poly(ethylene oxide). Polymer (Guildf). 2004;45(4):1235–42. https://doi.org/10.1016/j.polymer.2003.12.045.
61. Pielichowski K, Flejtuch K. Differential scanning calorimetry studies on poly(ethylene glycol) with different molecular weights for thermal energy storage materials. Polym Adv Technol. 2002;13(10–12):690–6. https://doi.org/10.1002/pat.276.
62. Pielichowski K, Flejtuch K. Differential scanning calorimetry study of blends of poly(ethylene glycol) with selected fatty acids. Macromol Mater Eng. 2003;288(3):259–64. https://doi.org/10.1002/mame.200390022.
63. Yan Q, Liang C. The thermal storage performance of monobasic, binary and triatomic polyalcohols systems. Sol Energy. 2008;82(7):656–62. https://doi.org/10.1016/J.SOLENER.2007.12.008.
64. Wang X, Lu E, Lin W, Wang C. Micromechanism of heat storage in a binary system of two kinds of polyalcohols as a solid-solid phase change material. Energy Convers Manag. 2000;41(2):135–44. https://doi.org/10.1016/S0196-8904(99)00096-5.
65. Feng H, Liu X, He S, Wu K, Zhang J. Studies on solid-solid phase transitions of polyols by infrared spectroscopy. Thermochim Acta. 2000;348(1–2):175–9. https://doi.org/10.1016/s0040-6031(99)00403-7.
66. Kim KB, Choi KW, Kim YJ, Lee KH, Lee KS. Feasibility study on a novel cooling technique using a phase change material in an automotive engine. Energy. 2010;35(1):478–84. https://doi.org/10.1016/J.ENERGY.2009.10.015.
67. Darkwa K, O'Callaghan PW. Green transport technology (GTT): analytical studies of a thermochemical store for minimising energy consumption and air pollution from automobile engines. Appl Therm Eng. 1997;17(7):603–14. https://doi.org/10.1016/S1359-4311(97)80001-4.
68. Gumus M. Reducing cold-start emission from internal combustion engines by means of thermal energy storage system. Appl Therm Eng. 2009;29(4):652–60. https://doi.org/10.1016/J.APPLTHERMALENG.2008.03.044.
69. Boam DJ. Energy audit on a two-litre saloon car driving an Ece 15 cycle from a cold start. Proc Inst Mech Eng Part D: Trans Eng. 1986;200(1):61–7. https://doi.org/10.1243/PIME_PROC_1986_200_164_02.
70. Schatz O. Cold start improvement by use of latent heat stores. SAE Tech Papers. 1992. https://doi.org/10.4271/921605.
71. Vasiliev LL, Burak VS, Kulakov AG, Mishkinis DA, Bohan PV. Latent heat storage modules for preheating internal combustion engines: application to a bus petrol engine. Appl Therm Eng. 2000;20(10):913–23. https://doi.org/10.1016/S1359-4311(99)00061-7.
72. Hong Y, Xin-shi G. Preparation of polyethylene-paraffin compound as a form-stable solid-liquid phase change material. Sol Energy Mater Sol Cells. 2000;64(1):37–44. https://doi.org/10.1016/S0927-0248(00)00041-6.
73. Sari A. Form-stable paraffin/high density polyethylene composites as solid-liquid phase change material for thermal energy storage: preparation and thermal properties. Energy Convers Manag. 2004;45(13–14):2033–42. https://doi.org/10.1016/j.enconman.2003.10.022.
74. Krupa I, Miková G, Luyt AS. Phase change materials based on low-density polyethylene/paraffin wax blends. Eur Polym J. 2007;43(11):4695–705. https://doi.org/10.1016/j.eurpolymj.2007.08.022.
75. Kaygusuz K, Sari A. High density polyethylene/paraffin composites as form-stable phase change material for thermal energy storage. Energy Sour Part A: Recover Util Environ Eff. 2007;29(3):261–70. https://doi.org/10.1080/009083190957568.
76. Biçer A, Sari A. New kinds of energy-storing building composite PCMs for thermal energy storage. Energy Convers Manag. 2013;69:148–56. https://doi.org/10.1016/J.ENCONMAN.2013.01.027.
77. Frigione M, Lettieri M, Sarcinella A. Phase change materials for energy efficiency in buildings and their use in mortars. Materials. 2019;12(8):1260. https://doi.org/10.3390/MA12081260.
78. Trinquet F, Karim L, Lefebvre G, Royon L. Mechanical properties and melting heat transfer characteristics of shape-stabilized paraffin slurry. Exp Heat Transf. 2013;27(1):1–13. https://doi.org/10.1080/08916152.2012.713076.
79. Jääskeläinen H, Majewski WA. Waste heat recovery for heavy-duty diesel engines: a review of mechanical turbocompounding. ASME 2017 Int Combust Engine Division Fall Tech Conf. 2017. https://doi.org/10.1115/ICEF2017-3695.
80. Zhao R, Zhuge W, Zhang Y, Yin Y, Li Z, Wang J. through flow matching of power turbine for a turbo-compounded diesel engine.

Proc ASME Turbo Expo. 2013;5:815–25. https://doi.org/10.1115/GT2012-69239.
81. Mamat AMI, Romagnoli A, Martinez-Botas RF. Design and development of a low pressure turbine for turbocompounding applications. Int J Gas Turbine Propuls Power Syst. 2012;4(3):1–8. https://doi.org/10.38036/JGPP.4.3_1.
82. Mamat AMI, Romagnoli A, Martinez-Botas RF. Characterisation of a low pressure turbine for turbocompounding applications in a heavily downsized mild-hybrid gasoline engine. Energy. 2014;64:3–16. https://doi.org/10.1016/J.ENERGY.2012.09.064.
83. Kruiswyk RW, Fairbanks J, Maronde C. An engine system approach to exhaust waste heat recovery. InDiesel Engine-Efficiency and Emissions Research (DEER) Conference, Dearborn, Michigan 2008.
84. Jung DH, Lee JK, Kim JY, Jang IS, Lee J, Lee HJ. Design method of an ultrahigh speed PM motor/generator for electric-turbo compounding system. IEEE Trans Appl Supercond. 2018;28(3):1–4. https://doi.org/10.1109/TASC.2018.2790917.
85. Comparison of high-speed PM machine topologies for electrically-assisted turbocharger applications. IEEE Conference PublicationIIEEE Xplore. Accessed on May 15, 2023. Available: https://ieeexplore.ieee.org/abstract/document/7837296
86. Lim MS, Kim JM, Hwang YS, Hong JP. Design of an ultra-high-speed permanent-magnet motor for an electric turbocharger considering speed response characteristics. IEEE/ASME Trans Mechatron. 2017;22(2):774–84. https://doi.org/10.1109/TMECH.2016.2634160.
87. Zhao R, Zhuge W, Zhang Y, Yin Y, Chen Z, Li Z. Parametric study of power turbine for diesel engine waste heat recovery. Appl Therm Eng. 2014;67(1–2):308–19. https://doi.org/10.1016/J.APPLTHERMALENG.2014.03.032.
88. Zhao R, Zhuge W, Zhang Y, Yang M, Martinez-Botas R, Yin Y. Study of two-stage turbine characteristic and its influence on turbo-compound engine performance. Energy Convers Manag. 2015;95:414–23. https://doi.org/10.1016/J.ENCONMAN.2015.01.079.
89. Zhao R, Li W, Zhuge W, Zhang Y, Yin Y. Numerical study on steam injection in a turbocompound diesel engine for waste heat recovery. Appl Energy. 2017;185:506–18. https://doi.org/10.1016/J.APENERGY.2016.10.135.
90. He GZ, Xie H, He SJ. Overall efficiency optimization of controllable mechanical turbo-compounding system for heavy duty diesel engines. Sci China Technol Sci. 2017;60(1):36–50. https://doi.org/10.1007/S11431-015-0754-6/METRICS.
91. Jääskeläinen H, Majewski WA. Waste heat recovery for heavy-duty diesel engines-a review of mechanical turbocompounding. ASME 2017 Int Combust Engine Division Fall Tech Conf. 2017;1:1–11. https://doi.org/10.1115/ICEF2017-3695.
92. Yamaguchi T, et al. Fundamental study of waste heat recovery in the high boosted 6-cylinder heavy duty diesel engine. SAE Int J Mater Manuf. 2015;8(2):209–26. https://doi.org/10.4271/2015-01-0326.
93. Ismail Y, Durrieu D, Menegazzi P, Chesse P, Chalet D. Potential of exhaust heat recovery by turbocompounding. SAE Tech Papers. 2012. https://doi.org/10.4271/2012-01-1603.
94. Ismail Y, Durrieu D, Menegazzi P, Chesse P, Chalet D. Study of parallel turbocompounding for small displacement engines. SAE Tech Papers. 2013. https://doi.org/10.4271/2013-01-1637.
95. Cipollone R, Di Battista D, Gualtieri A. Turbo compound systems to recover energy in ICE. Int J Eng Innov Technol (IJEIT). 2013;3(6):249–57.
96. Mamat AMIB, Martinez-Botas RF, Chiong MC, Rajoo S, Petrovic S, Romagnoli A. Exhaust gas energy recovery via electric turbocompounding. Energy Procedia. 2015;75:1555–9. https://doi.org/10.1016/j.egypro.2015.07.336.
97. Wasselin T, Richard S, Berr F, Dabadie JC, Alix G. Potential of several alternative propulsion systems for light rotorcrafts applications. SAE Int J Aerosp. 2013;6(2):563–70. https://doi.org/10.4271/2013-01-2230.
98. He G, Xie H. Fuel saving potential of different turbo-compounding systems under steady and driving cycles. SAE Tech Papers. 2015. https://doi.org/10.4271/2015-01-0878.
99. Salehi R, Kiwan R, Martz J, Stefanopoulou AG. Design considerations for waste energy recovery with electric turbocompounding. ASME 2016 Dyn Syst Control Conf. 2016. https://doi.org/10.1115/DSCC2016-9819.
100. Law CL, Joardder MU, Masud MH, Karim MA. Relationship between intermittency of drying, microstructural changes, and food quality. Intermittent Nonstation Dry Technol. 2017. https://doi.org/10.4324/9781351251303-6.
101. Chen G. Agricultural and forestry product drying operations. Encycl Energy Eng Technol. 2014. https://doi.org/10.1081/E-EEE2-120042965.
102. Zarein M, Samadi SH, Ghobadian B. Investigation of microwave dryer effect on energy efficiency during drying of apple slices. J Saudi Soc Agric Sci. 2015;14(1):41–7. https://doi.org/10.1016/J.JSSAS.2013.06.002.
103. Joardder MUH, Masud MH. Food preservation in developing countries: Challenges and solutions. Food Preserv Dev Ctries: Chall Solut. 2019. https://doi.org/10.1007/978-3-030-11530-2/COVER.
104. Masud MH, Himel HH, Arefin AME, Ananno AA, Rashid M, Dabnichki P. Mathematical modelling and exergo-environmental analysis of drying potato samples in a waste heat-based convective dryer. Environ Chall. 2021;5(November):2–11. https://doi.org/10.1016/j.envc.2021.100372.
105. Kara C, Doymaz İ. Effective moisture diffusivity determination and mathematical modelling of drying curves of apple pomace. Heat Mass Transf/Waerme-und Stoffuebertragung. 2015;51(7):983–9. https://doi.org/10.1007/s00231-014-1470-6.
106. Wang Z, et al. Mathematical modeling on hot air drying of thin layer apple pomace. Food Res Int. 2007;40(1):39–46. https://doi.org/10.1016/j.foodres.2006.07.017.
107. Roberts JS, Kidd DR, Padilla-Zakour O. Drying kinetics of grape seeds. J Food Eng. 2008;89(4):460–5. https://doi.org/10.1016/j.jfoodeng.2008.05.030.
108. Sharma SR, Arora S, Chand T. Air drying kinetics of pomegranate seeds. Int J Food Eng. 2011. https://doi.org/10.2202/1556-3758.1691.
109. Celma AR, Rojas S, López F, Montero I, Miranda T. Thin-layer drying behaviour of sludge of olive oil extraction. J Food Eng. 2007;80(4):1261–71. https://doi.org/10.1016/j.jfoodeng.2006.09.020.
110. Kumar N, Sarkar BC, Sharma HK. Mathematical modelling of thin layer hot air drying of carrot pomace. J Food Sci Technol. 2012;49(1):33–41. https://doi.org/10.1007/s13197-011-0266-7.
111. Murugavelh S, Anand B, Midhun Prasad K, Nagarajan R, Azariah Pravin Kumar S. Exergy analysis and kinetic study of tomato waste drying in a mixed mode solar tunnel dryer. Energy Sour Part A Recover Util Environ Eff. 2019. https://doi.org/10.1080/15567036.2019.1679289.
112. Pathare PB, Sharma GP. Effective moisture diffusivity of onion slices undergoing infrared convective drying. Biosyst Eng. 2006;93(3):285–91. https://doi.org/10.1016/j.biosystemseng.2005.12.010.
113. Toğrul H. Suitable drying model for infrared drying of carrot. J Food Eng. 2006;77(3):610–9. https://doi.org/10.1016/j.jfoodeng.2005.07.020.

114. Doymaz I. Convective air drying characteristics of thin layer carrots. J Food Eng. 2004;61(3):359–64. https://doi.org/10.1016/S0260-8774(03)00142-0.
115. Sadeghi M, Mirzabeigi Kesbi O, Mireei SA. Mass transfer characteristics during convective, microwave and combined microwave–convective drying of lemon slices. J Sci Food Agric. 2013;93(3):471–8. https://doi.org/10.1002/JSFA.5786.
116. Talens C, Castro-Giraldez M, Fito PJ. Effect of microwave power coupled with hot air drying on sorption isotherms and microstructure of orange peel. Food Bioproc Tech. 2018;11(4):723–34. https://doi.org/10.1007/S11947-017-2041-X/METRICS.
117. Horrungsiwat S, Therdthai N, Ratphitagsanti W. Effect of combined microwave-hot air drying and superheated steam drying on physical and chemical properties of rice. Int J Food Sci Technol. 2016;51(8):1851–9. https://doi.org/10.1111/IJFS.13157.
118. Nuthong P, Achariyaviriya A, Namsanguan K, Achariyaviriya S. Kinetics and modeling of whole longan with combined infrared and hot air. J Food Eng. 2011;102(3):233–9.
119. El-Mesery HS, Mwithiga G. Performance of a convective, infrared and combined infrared- convective heated conveyor-belt dryer. J Food Sci Technol. 2015;52(5):2721–30. https://doi.org/10.1007/S13197-014-1347-1/METRICS.
120. Mihindukulasuriya SDF, Jayasuriya HPW. Drying of chilli in a combined infrared and hot air rotary dryer. J Food Sci Technol. 2015;52(8):4895–904. https://doi.org/10.1007/S13197-014-1546-9/METRICS.
121. Tuncel NB, Onsekiz Ç, Üniversitesi M, Öztürk N. The effects of infrared and hot air drying on some properties of corn (Zea mays). J Food Agric Environ. 2010;8(1):63–8.
122. Zare D, Naderi H, Ranjbaran M. Energy and quality attributes of combined hot-air/infrared drying of paddy. Drying Technol. 2015;33(5):570–82. https://doi.org/10.1080/07373937.2014.962143.
123. Wang Y, et al. Developing hot air-assisted radio frequency drying for in-shell macadamia nuts. Food Bioproc Tech. 2014;7(1):278–88. https://doi.org/10.1007/S11947-013-1055-2/METRICS.
124. Shinde A, Das S, Datta AK. Quality improvement of orthodox and CTC tea and performance enhancement by hybrid hot air–radio frequency (RF) dryer. J Food Eng. 2013;116(2):444–9. https://doi.org/10.1016/J.JFOODENG.2012.12.001.
125. Sadeghi M, Mirzabeigi Kesbi O, Mireei SA. Mass transfer characteristics during convective, microwave and combined microwave-convective drying of lemon slices. J Sci Food Agric. 2013;93(3):471–8.
126. Yousefi A, Niakousari M, Moradi M. Microwave assisted hot air drying of papaya (*Carica papaya* L.) pretreated in osmotic solution. Afr J Agric Res. 2013;8(25):3229–35. https://doi.org/10.5897/AJAR12.180.
127. El-Mesery HS, Mwithiga G. Performance of a convective, infrared and combined infrared-convective heated conveyor-belt dryer. J Food Sci Technol. 2015;52(5):2721–30. https://doi.org/10.1007/s13197-014-1347-1.
128. Tuncel NB, Yilmaz N, Kocabiyik H, Öztürk N, Tunçel M. The effects of infrared and hot air drying on some properties of corn (Zea mays). J Food Agric Environ. 2010;8(1):63–8.
129. Motevali A, Minaei S, Khoshtaghaza MH, Amirnejat H. Comparison of energy consumption and specific energy requirements of different methods for drying mushroom slices. Energy. 2011;36(11):6433–41. https://doi.org/10.1016/j.energy.2011.09.024.
130. Shinde A, Das S, Datta AK. Quality improvement of orthodox and CTC tea and performance enhancement by hybrid hot air-radio frequency (RF) dryer. J Food Eng. 2013;116(2):444–9. https://doi.org/10.1016/j.jfoodeng.2012.12.001.
131. Chiranjeevi C, Srinivas T. Exergy analysis of dehumidifier in a combined two stage desalination and cooling plant. Des. 2014;345(3):56–63.
132. Singh M, Jaiswal N. Dehumidifiers for chronic asthma. Cochrane Database Syst Rev. 2013;6:CD003563. https://doi.org/10.1002/14651858.CD003563.PUB2.
133. Applications of a commercial dehumidifier and how they work-EHUM- engineering dry air. Accessed on May 17, 2023. Available: https://www.dehum.com/news/commercial-dehumidifier
134. What is Dehumidifier? meaning, advantages & types—electricalworkbook. Accessed on May 17, 2023. Available: https://electricalworkbook.com/dehumidifier/
135. How does a dehumidifier work//mitsubishi electric. Accessed on May 17, 2023. Available: https://www.mitsubishi-electric.co.nz/dehumidifier/how.aspx
136. Wasserautarke Gewächshäuser durch Nutzung von Sonnenenergie (2012) Accessed on May 17, 2023. Available: https://patents.google.com/patent/DE102012014560A1/pt-pt
137. Hasan MA, Sumathy K. Photovoltaic thermal module concepts and their performance analysis: a review. Renew Sustain Energy Rev. 2010;14(7):1845–59. https://doi.org/10.1016/j.rser.2010.03.011.
138. Brogren M, Karlsson B. Low-concentrating water-cooled PV-thermal hybrid systems for high latitudes. Conf Rec IEEE Photovolt Spec Conf. 2002. https://doi.org/10.1109/pvsc.2002.1190956.
139. El Chammas R, Clodic D. Combined cycle for hybrid vehicles. SAE Tech Papers. 2005. https://doi.org/10.4271/2005-01-1171.
140. Zondag HA. Flat-plate PV-Thermal collectors and systems: a review. Renew Sustain Energy Rev. 2008;12(4):891–959. https://doi.org/10.1016/j.rser.2005.12.012.
141. Cox CH, Raghuraman P. Design considerations for flat-plate-photovoltaic/thermal collectors. Sol Energy. 1985;35(3):227–41. https://doi.org/10.1016/0038-092X(85)90102-1.
142. Lalović B, Kiss Z, Weakliem H. A hybrid amorphous silicon photovoltaic and thermal solar collector. Solar Cells. 1986;19(2):131–8. https://doi.org/10.1016/0379-6787(86)90038-4.
143. Garg HP, Agarwal RK. Some aspects of a PV/T collector/forced circulation flat plate solar water heater with solar cells. Energy Convers Manag. 1995;36(2):87–99. https://doi.org/10.1016/0196-8904(94)00046-3.
144. Huang BJ, Du SC. A performance test method of solar thermosyphon systems. J Sol Energy Eng. 1991;113(3):172–9. https://doi.org/10.1115/1.2930489.
145. Wolf M. Performance analyses of combined heating and photovoltaic power systems for residences. Energy Conversion. 1976;16(1–2):79–90. https://doi.org/10.1016/0013-7480(76)90018-8.
146. Zondag HA, De Vries DW, Van Helden WGJ, Van Zolingen RJC, Van Steenhoven AA. The thermal and electrical yield of a PV-thermal collector. Sol Energy. 2002;72(2):113–28. https://doi.org/10.1016/S0038-092X(01)00094-9.
147. Zondag HA, de Vries DW, van Helden WGJ, van Zolingen RJC, van Steenhoven AA. The yield of different combined PV-thermal collector designs. Sol Energy. 2003;74(3):253–69. https://doi.org/10.1016/S0038-092X(03)00121-X.
148. Bakker M, Zondag HA, Elswijk MJ, Strootman KJ, Jong MJM. Performance and costs of a roof-sized PV/thermal array combined with a ground coupled heat pump. Sol Energy. 2005;78(2):331–9. https://doi.org/10.1016/J.SOLENER.2004.09.019.
149. Vokas G, Christandonis N, Skittides F. Hybrid photovoltaic–thermal systems for domestic heating and cooling—a theoretical approach. Sol Energy. 2006;80(5):607–15. https://doi.org/10.1016/J.SOLENER.2005.03.011.

150. Assoa YB, Menezo C, Fraisse G, Yezou R, Brau J. Study of a new concept of photovoltaic-thermal hybrid collector. Sol Energy. 2007;81(9):1132–43. https://doi.org/10.1016/j.solener.2007.04.001.
151. Tripanagnostopoulos Y. Aspects and improvements of hybrid photovoltaic/thermal solar energy systems. Sol Energy. 2007;81(9):1117–31. https://doi.org/10.1016/j.solener.2007.04.002.
152. Dubey S, Tiwari GN. Analysis of PV/T flat plate water collectors connected in series. Sol Energy. 2009;83(9):1485–98. https://doi.org/10.1016/j.solener.2009.04.002.
153. Dubey S, Tiwari GN. Thermal modeling of a combined system of photovoltaic thermal (PV/T) solar water heater. Sol Energy. 2008;82(7):602–12. https://doi.org/10.1016/j.solener.2008.02.005.
154. Ibrahim A, et al. Performance of photovoltaic thermal collector (PVT) with different absorbers design. WSEAS Trans Environ Dev. 2009;5(3):321–30.
155. Boubekri M, Chaker A, Cheknane A. Numerical approach for performance study of hybrid PV/Thermal collector. Revue des Energies Renouvelables. 2009;12:3–355.
156. da Silva RM, Fernandes JLM. Hybrid photovoltaic/thermal (PV/T) solar systems simulation with Simulink/Matlab. Sol Energy. 2010;84(12):1985–96. https://doi.org/10.1016/j.solener.2010.10.004.
157. He W, Zhang Y, Ji J. Comparative experiment study on photovoltaic and thermal solar system under natural circulation of water. Appl Therm Eng. 2011;31(16):3369–76. https://doi.org/10.1016/j.applthermaleng.2011.06.021.
158. Dupeyrat P, Ménézo C, Rommel M, Henning HM. Efficient single glazed flat plate photovoltaic-thermal hybrid collector for domestic hot water system. Sol Energy. 2011;85(7):1457–68. https://doi.org/10.1016/j.solener.2011.04.002.
159. Gang P, Huide F, Tao Z, Jie J. A numerical and experimental study on a heat pipe PV/T system. Sol Energy. 2011;85(5):911–21. https://doi.org/10.1016/j.solener.2011.02.006.
160. Malvi CS, Dixon-Hardy DW, Crook R. Energy balance model of combined photovoltaic solar-thermal system incorporating phase change material. Sol Energy. 2011;85(7):1440–6. https://doi.org/10.1016/j.solener.2011.03.027.
161. Charalambous PG, Kalogirou SA, Maidment GG, Yiakoumetti K. Optimization of the photovoltaic thermal (PV/T) collector absorber. Sol Energy. 2011;85(5):871–80. https://doi.org/10.1016/j.solener.2011.02.003.
162. Crane D, Jackson G, Holloway D. towards optimization of automotive waste heat recovery using thermoelectrics. SAE Tech Papers. 2001. https://doi.org/10.4271/2001-01-1021.
163. Koutroulis E, Kalaitzakis K, Voulgaris NC. Development of a microcontroller-based, photovoltaic maximum power point tracking control system. IEEE Trans Power Electron. 2001;16(1):46–54. https://doi.org/10.1109/63.903988.
164. Zheng S, Liu W (2008) Research and implementation of photovoltaic charging system with maximum power point tracking. In: 2008 3rd IEEE conference on industrial electronics and applications, ICIEA 2008, pp 619–624. https://doi.org/10.1109/ICIEA.2008.4582589.
165. Chowdhury S, Jakaria Rahimi M, Riazul Hamid M, Rahimi J, Moniruzzaman Sunny T. Design and development of a maximum power point tracking (MPPT) charge controller for photovoltaic (PV) power generation system. Am J Eng Res (AJER). 2016;5(5):15–22.
166. Pradhan A, Panda B. A simplified design and modeling of boost converter for photovoltaic sytem. Int J Electr Comput Eng. 2018;8(1):141–9. https://doi.org/10.11591/ijece.v8i1.pp141-149.
167. Liu Y. Power point tracking battery charging system. Small. 2005;3(1):1–5.
168. Sani F, Yahya HN, Momoh M, Saidu IG, Akpootu DO. Design and construction of microcontroller based charge controller for photovoltaic application. IOSR J Electr Electron Eng. 2014;9(1):92–7. https://doi.org/10.9790/1676-09119297.
169. Bullock KR. Carbon reactions and effects on valve-regulated lead-acid (VRLA) battery cycle life in high-rate, partial state-of-charge cycling. J Power Sour. 2010;195(14):4513–9. https://doi.org/10.1016/J.JPOWSOUR.2009.10.027.
170. Feizi T, Kwiecien M, Sauer DU (2016) Analysis of characteristics for the identification of lead-acid battery technologies used in micro-hybrid vehicles. In: EEEIC 2016 international conference on environment and electrical engineering. https://doi.org/10.1109/EEEIC.2016.7555656.
171. Li Y, Song J, Yang J. A review on structure model and energy system design of lithium-ion battery in renewable energy vehicle. Renew Sustain Energy Rev. 2014;37:627–33. https://doi.org/10.1016/j.rser.2014.05.059.
172. Zamarayeva AM, et al. Fabrication of a high-performance flexible silver-zinc wire battery. Adv Electron Mater. 2016;2(5):1–7. https://doi.org/10.1002/aelm.201500296.
173. Smeacetto F, et al. Glass-ceramic joining material for sodium-based battery. Ceram Int. 2017;43(11):8329–33. https://doi.org/10.1016/j.ceramint.2017.03.170.
174. Andriollo M, et al. Energy intensive electrochemical storage in Italy: 34.8 MW sodium-sulphur secondary cells. J Energy Storage. 2016;5:146–55. https://doi.org/10.1016/j.est.2015.12.003.
175. Chikkannanavar SB, Bernardi DM, Liu L. A review of blended cathode materials for use in Li-ion batteries. J Power Sources. 2014;248:91–100. https://doi.org/10.1016/j.jpowsour.2013.09.052.
176. Massaguer A, et al. Transient behavior under a normalized driving cycle of an automotive thermoelectric generator. Appl Energy. 2017;206:1282–96. https://doi.org/10.1016/J.APENERGY.2017.10.015.
177. Li B, Huang K, Yan Y, Li Y, Twaha S, Zhu J. Heat transfer enhancement of a modularised thermoelectric power generator for passenger vehicles. Appl Energy. 2017;205:868–79. https://doi.org/10.1016/J.APENERGY.2017.08.092.
178. Wang Y, Dai C, Wang S. Theoretical analysis of a thermoelectric generator using exhaust gas of vehicles as heat source. Appl Energy. 2013;112:1171–80. https://doi.org/10.1016/J.APENERGY.2013.01.018.
179. Sun Y, Di CA, Xu W, Zhu D. Advances in n-type organic thermoelectric materials and devices. Adv Electron Mater. 2019;5(11):1800825. https://doi.org/10.1002/AELM.201800825.
180. Tani JI, Kido H. Thermoelectric properties of Bi-doped Mg2Si semiconductors. Physica B Condens Matter. 2005;364(1–4):218–24. https://doi.org/10.1016/J.PHYSB.2005.04.017.
181. Zhu Y, Wang C, Wang H, Su W, Liu J, Li J. Influence of Dy/Bi dual doping on thermoelectric performance of CaMnO3 ceramics. Mater Chem Phys. 2014;144(3):385–9. https://doi.org/10.1016/J.MATCHEMPHYS.2014.01.006.
182. Yasukawa M, Kono T, Ueda K, Yanagi H, Hosono H. High-temperature thermoelectric properties of La-doped BaSnO3 ceramics. Mater Sci Eng, B. 2010;173(1–3):29–32. https://doi.org/10.1016/J.MSEB.2009.10.002.
183. Wang S, et al. High-temperature thermoelectric properties of Cd1−xPrxO ceramics. Scr Mater. 2013;69(7):533–6. https://doi.org/10.1016/J.SCRIPTAMAT.2013.06.018.
184. Tsubota T, Ohno T, Shiraishi N, Miyazaki Y. Thermoelectric properties of Sn1−x−yTiySbxO2 ceramics. J Alloys Compd. 2008;463(1–2):288–93. https://doi.org/10.1016/J.JALLCOM.2007.09.001.

185. Li X, et al. Experimental investigation on a thermoelectric cooler for thermal management of a lithium-ion battery module. Int J Photoenergy. 2019. https://doi.org/10.1155/2019/3725364.
186. Sabir B, Murtaza G, Arif Khalil RM, Mahmood Q. First principle study of electronic, mechanical, optical and thermoelectric properties of CsMO3 (M = Ta, Nb) compounds for optoelectronic devices. J Mol Graph Model. 2019;86:19–26. https://doi.org/10.1016/J.JMGM.2018.09.011.
187. Wang L, Wang D, Zhu G, Li J, Pan F. Thermoelectric properties of conducting polyaniline/graphite composites. Mater Lett. 2011;65(7):1086–8. https://doi.org/10.1016/J.MATLET.2011.01.014.
188. Elmoughni HM, Menon AK, Wolfe RMW, Yee SK. A textile-integrated polymer thermoelectric generator for body heat harvesting. Adv Mater Technol. 2019;4(7):1800708. https://doi.org/10.1002/ADMT.201800708.
189. Lu Y, Wang JY, Pei J. Strategies to enhance the conductivity of n-type polymer thermoelectric materials. Chem Mater. 2019;31(17):6412–23. https://doi.org/10.1021/ACS.CHEMMATER.9B01422/ASSET/IMAGES/MEDIUM/CM-2019-01422W_0011.GIF.
190. Pang H, Piao YY, Tan YQ, Jiang GY, Wang JH, Li ZM. Thermoelectric behaviour of segregated conductive polymer composites with hybrid fillers of carbon nanotube and bismuth telluride. Mater Lett. 2013;107:150–3. https://doi.org/10.1016/J.MATLET.2013.06.008.
191. Tan M, Hao Y, Wang G. Improvement of thermoelectric properties induced by uniquely ordered lattice field in Bi2Se0.5Te2.5 pillar array. J Solid State Chem. 2014;215:219–24. https://doi.org/10.1016/j.jssc.2014.04.005.
192. Yeo YH, Oh TS. Thermoelectric properties of p-type (Bi, Sb)2Te3 nanocomposites dispersed with multiwall carbon nanotubes. Mater Res Bull. 2014;58:54–8. https://doi.org/10.1016/j.materresbull.2014.04.046.
193. Chen Z, Lin MY, Xu GD, Chen S, Zhang JH, Wang MM. Hydrothermal synthesized nanostructure Bi-Sb-Te thermoelectric materials. J Alloys Compd. 2014;588:384–7. https://doi.org/10.1016/j.jallcom.2013.11.065.
194. Fan X, Cai X, Rong Z, Yang F, Li G, Gan Z. Resistance pressing sintering: a simple, economical and practical technique and its application to p-type (Bi, Sb)$_2$Te$_3$ thermoelectric materials. J Alloys Compd. 2014;607:91–8. https://doi.org/10.1016/j.jallcom.2014.04.032.
195. Tan M, Deng Y, Wang Y. Ordered structure and high thermoelectric properties of Bi2(Te, Se)$_3$ nanowire array. Nano Energy. 2014;3:144–51. https://doi.org/10.1016/j.nanoen.2013.07.009.
196. Xu Z, Yang J, Xiao Y, Li G, Zhang JS, Peng J. Thermoelectric properties of P-type(Bi0.26Sb0.74) 2Te3+3%Te ingots prepared by vacuum melting. Procedia Eng. 2012;27(2011):137–43. https://doi.org/10.1016/j.proeng.2011.12.435.
197. Jiang J, Chen L, Bai S, Yao Q. Thermoelectric performance of p-type Bi–Sb–Te materials prepared by spark plasma sintering. J Alloys Compd. 2005;390(1–2):208–11. https://doi.org/10.1016/j.jallcom.2004.07.056.
198. Hong SJ, Lee SH, Chun BS. Thermoelectric properties of newly fabricated n-type 95%Bi2Te2-5%Bi2Se3 alloys by gas atomizing and extrusion process. Mater Sci Eng B Solid State Mater Adv Technol. 2003;98(3):232–8. https://doi.org/10.1016/S0921-5107(03)00042-4.
199. Park K, Seo JH, Cho DC, Choi BH, Lee CH. Thermoelectric properties of p-type Te doped Bi0.5Sb1.5Te3 fabricated by powder extrusion. Mater Sci Eng B Solid State Mater Adv Technol. 2002;88(1):103–6. https://doi.org/10.1016/S0921-5107(01)00912-6.
200. Yang JY, Aizawa T, Yamamoto A, Ohta T. Effects of interface layer on thermoelectric properties of a pn junction prepared via the BMA-HP method. Mater Sci Eng B Solid State Mater Adv Technol. 2001;85(1):34–7. https://doi.org/10.1016/S0921-5107(01)00630-4.
201. Yang JY, Aizawa T, Yamamoto A, Ohta T. Thermoelectric properties of n-type (Bi2Se3)x(Bi2Te3)1–x prepared by bulk mechanical alloying and hot pressing. J Alloys Compd. 2000;312(1–2):326–30. https://doi.org/10.1016/S0925-8388(00)01159-2.
202. Seo J-H, Lee D-M, Lee C-H, Park K, Kim J-H, Nishida IA. Microstructural and thermoelectric properties of hot-extruded p-type Bi0.5Sb1.5Te3. Cambridge: Woodhead Publishing Limited; 1997.
203. Otake M, Sato K, Sugiyama O, Kaneko S. Pulse-current sintering and thermoelectric properties of gas-atomized silicon-germanium powders. Solid State Ion. 2004;172(1–4):523–6. https://doi.org/10.1016/j.ssi.2004.01.056.
204. Venkatasubramanian R, et al. Thin-film thermoelectric devices with high room-temperature figures of merit. Nature. 2001;413(6856):597–602.
205. Tang ZB, Deng YD, Su CQ, Shuai WW, Xie CJ. A research on thermoelectric generator's electrical performance under temperature mismatch conditions for automotive waste heat recovery system. Case Stud Therm Eng. 2015;5:143–50. https://doi.org/10.1016/J.CSITE.2015.03.006.
206. Wilbrecht S, Beitelschmidt M. The potential of a cascaded teg system for waste heat usage in railway vehicles. J Electron Mater. 2018;47(6):3358–69. https://doi.org/10.1007/S11664-018-6094-Z/METRICS.
207. Dhathathreyan KS, et al. Development of polymer electrolyte membrane fuel cell stack. Int J Hydrogen Energy. 1999;24(11):1107–15. https://doi.org/10.1016/S0360-3199(98)00172-4.
208. Kordesch KV. 25 years of fuel cell development (1951–1976). J Electrochem Soc. 1978;125(3):77C-88C. https://doi.org/10.1149/1.2131782.
209. Fuel cell handbook (Book)|OSTI.GOV. Accessed on May 18, 2023. Available: https://www.osti.gov/biblio/5616450
210. Wilberforce T, Ijaodola O, Ogungbemi E, El Hassan Z, Thompson J, Olabi AG. Effect of bipolar plate materials on performance of fuel cells. Ref Modul Mater Sci Mater Eng. 2018. https://doi.org/10.1016/B978-0-12-803581-8.11272-X.
211. Hermann A, Chaudhuri T, Spagnol P. Bipolar plates for PEM fuel cells: a review. Int J Hydrog Energy. 2005;30(12):1297–302. https://doi.org/10.1016/J.IJHYDENE.2005.04.016.
212. Alaswad A, et al. Technical and commercial challenges of proton-exchange membrane (PEM) fuel cells. Energies. 2020;14(1):144. https://doi.org/10.3390/EN14010144.
213. Litster S, McLean G. PEM fuel cell electrodes. J Power Sour. 2004;130(1–2):61–76. https://doi.org/10.1016/J.JPOWSOUR.2003.12.055.
214. Velasco Martínez A, et al. Pd and Pd-Co oxygen reduction nanocatalysts in acidic media. Int J Electrochem Sci. 2012;7:7140–51.
215. Zhong J, et al. Synthesis and high electrocatalytic activity of Au-decorated Pd heterogeneous nanocube catalysts for ethanol electro-oxidation in alkaline media. Catal Sci Technol. 2016;6(14):5397–404. https://doi.org/10.1039/C6CY00140H.
216. Musto P, Karasz FE, MacKnight WJ. Fourier transform infra-red spectroscopy on the thermo-oxidative degradation of polybenzimidazole and of a polybenzimidazole/polyetherimide blend. Polymer (Guildf). 1993;34(14):2934–45. https://doi.org/10.1016/0032-3861(93)90618-K.
217. Tan J, Chao YJ, Yang M, Lee WK, Van Zee JW. Chemical and mechanical stability of a Silicone gasket material exposed to PEM fuel cell environment. Int J Hydrog Energy.

2011;36(2):1846–52. https://doi.org/10.1016/J.IJHYDENE.2009.12.048.
218. Li Z, et al. Enhanced proton conductivity of nafion hybrid membrane under different humidities by incorporating metal-organic frameworks with high phytic acid loading. ACS Appl Mater Interfaces. 2014;6(12):9799–807. https://doi.org/10.1021/am502236v.
219. Matsumura S, et al. Stability and utility of pyridyl disulfide functionality in RAFT and conventional radical polymerizations. J Polym Sci A Polym Chem. 2008;46(April):7207–24. https://doi.org/10.1002/pola.
220. Kumar R, Xu C, Scott K. Graphite oxide/Nafion composite membranes for polymer electrolyte fuel cells. RSC Adv. 2012;2(23):8777–82. https://doi.org/10.1039/c2ra20225e.
221. Nam SE, Kim SO, Kang Y, Lee JW, Lee KH. Preparation of Nafion/sulfonated poly(phenylsilsesquioxane) nanocomposite as high temperature proton exchange membranes. J Memb Sci. 2008;322(2):466–74. https://doi.org/10.1016/j.memsci.2008.05.075.
222. Patel HA, Mansor N, Gadipelli S, Brett DJL, Guo Z. Superacidity in nafion/mof hybrid membranes retains water at low humidity to enhance proton conduction for fuel cells. ACS Appl Mater Interfaces. 2016;8(45):30687–91. https://doi.org/10.1021/acsami.6b12240.
223. Kongkachuichay P, Pimprom S. Nafion/analcime and nafion/faujasite composite membranes for high temperature operation of PEMFC. Proc World Congr Eng Comput Sci. 2008;2008:1–5.
224. Yang L, Tang B, Wu P. Metal-organic framework-graphene oxide composites: a facile method to highly improve the proton conductivity of PEMs operated under low humidity. J Mater Chem A Mater. 2015;3(31):15838–42. https://doi.org/10.1039/c5ta03507d.
225. Rao Z, Tang B, Wu P. Proton conductivity of proton exchange membrane synergistically promoted by different functionalized metal-organic frameworks. ACS Appl Mater Interfaces. 2017;9(27):22597–603. https://doi.org/10.1021/acsami.7b05969.
226. Sahu AK, Ketpang K, Shanmugam S, Kwon O, Lee S, Kim H. Sulfonated graphene-nafion composite membranes for polymer electrolyte fuel cells operating under reduced relative humidity. J Phys Chem C. 2016;120(29):15855–66. https://doi.org/10.1021/acs.jpcc.5b11674.
227. Vinothkannan M, Kim AR, Gnana Kumar G, Yoo DJ. Sulfonated graphene oxide/Nafion composite membranes for high temperature and low humidity proton exchange membrane fuel cells. RSC Adv. 2018;8(14):7494–508. https://doi.org/10.1039/c7ra12768e.
228. Shao ZG, Xu H, Li M, Hsing IM. Hybrid Nafion-inorganic oxides membrane doped with heteropolyacids for high temperature operation of proton exchange membrane fuel cell. Solid State Ion. 2006;177(7–8):779–85. https://doi.org/10.1016/j.ssi.2005.12.035.
229. Lu JL, Fang QH, Li SL, Jiang SP. A novel phosphotungstic acid impregnated meso-Nafion multilayer membrane for proton exchange membrane fuel cells. J Memb Sci. 2013;427:101–7. https://doi.org/10.1016/j.memsci.2012.09.041.
230. Samms SR, Wasmus S, Savinell RF. Thermal stability of proton conducting acid doped polybenzimidazole in simulated fuel cell environments. J Electrochem Soc. 1996;143(4):1225–32. https://doi.org/10.1149/1.1836621.
231. Zhang J, Tang Y, Song C, Zhang J. Polybenzimidazole-membrane-based PEM fuel cell in the temperature range of 120–200 °C. J Power Sour. 2007;172(1):163–71. https://doi.org/10.1016/j.jpowsour.2007.07.047.
232. Ergun D, Devrim Y, Bac N, Eroglu I. Phosphoric acid doped polybenzimidazole membrane for high temperature PEM fuel cell. J Appl Polym Sci. 2012;124(SUPPL. 1):2015–6. https://doi.org/10.1002/app.36507.
233. Wieser C. Novel polymer electrolyte membranes for automotive applications—requirements and benefits. Fuel Cells. 2004;4(4):245–50. https://doi.org/10.1002/fuce.200400038.
234. Zhang J, et al. High temperature PEM fuel cells. J Power Sour. 2006. https://doi.org/10.1016/j.jpowsour.2006.05.034.
235. Wee JH. Applications of proton exchange membrane fuel cell systems. Renew Sustain Energy Rev. 2007;11(8):1720–38. https://doi.org/10.1016/j.rser.2006.01.005.
236. Wan Z, Chang H, Shu S, Wang Y, Tang H. A review on cold start of proton exchange membrane fuel cells. Energies. 2014;7:3179–203. https://doi.org/10.3390/EN7053179.
237. Alizadeh E, Rahgoshay SM, Rahimi-Esbo M, Khorshidian M, Saadat SHM. A novel cooling flow field design for polymer electrolyte membrane fuel cell stack. Int J Hydrog Energy. 2016;41(20):8525–32. https://doi.org/10.1016/j.ijhydene.2016.03.187.
238. Zhang G, Kandlikar SG. A critical review of cooling techniques in proton exchange membrane fuel cell stacks. Int J Hydrog Energy. 2012;37(3):2412–29. https://doi.org/10.1016/j.ijhydene.2011.11.010.
239. Lehner M, Tichler R, Koppe M. Power-to-gas: technology and business models. Cham: Springer; 2014.
240. Laguna-Bercero MA. Recent advances in high temperature electrolysis using solid oxide fuel cells: a review. J Power Sour. 2012;203:4–16. https://doi.org/10.1016/j.jpowsour.2011.12.019.
241. Conte M, Di Mario F, Iacobazzi A, Mattucci A, Moreno A, Ronchetti M. Hydrogen as future energy carrier: the ENEA point of view on technology and application prospects. Energies (Basel). 2009;2(1):150–79. https://doi.org/10.3390/en20100150.
242. Carmo M, Fritz DL, Mergel J, Stolten D. A comprehensive review on PEM water electrolysis. Int J Hydrog Energy. 2013;38(12):4901–34. https://doi.org/10.1016/j.ijhydene.2013.01.151.
243. Sapountzi FM, Gracia JM, Fredriksson HO, Niemantsverdriet JH. Electrocatalysts for the generation of hydrogen, oxygen and synthesis gas. Prog Energy Combust Sci. 2017;58:1–35. https://doi.org/10.1016/j.pecs.2016.09.001.
244. Nikolaidis P, Poullikkas A. A comparative overview of hydrogen production processes. Renew Sustain Energy Rev. 2017;67:597–611. https://doi.org/10.1016/J.RSER.2016.09.044.
245. Shiva Kumar S, Himabindu V. Hydrogen production by PEM water electrolysis—a review. Mater Sci Energy Technol. 2019;2(3):442–54. https://doi.org/10.1016/j.mset.2019.03.002.
246. Lædre S, Kongstein OE, Oedegaard A, Karoliussen H, Seland F. Materials for proton exchange membrane water electrolyzer bipolar plates. Int J Hydrog Energy. 2017;42(5):2713–23. https://doi.org/10.1016/J.IJHYDENE.2016.11.106.
247. Majasan JO, Cho JIS, Dedigama I, Tsaoulidis D, Shearing P, Brett DJL. Two-phase flow behaviour and performance of polymer electrolyte membrane electrolysers: electrochemical and optical characterisation. Int J Hydrog Energy. 2018;43(33):15659–72. https://doi.org/10.1016/J.IJHYDENE.2018.07.003.
248. Corrales-Sánchez T, Ampurdanés J, Urakawa A. MoS2-based materials as alternative cathode catalyst for PEM electrolysis. Int J Hydrog Energy. 2014;39(35):20837–43. https://doi.org/10.1016/j.ijhydene.2014.08.078.
249. Ng JWD, Hellstern TR, Kibsgaard J, Hinckley AC, Benck JD, Jaramillo TF. Polymer electrolyte membrane electrolyzers utilizing non-precious mo-based hydrogen evolution catalysts. Chemsuschem. 2015;8(20):3512–9. https://doi.org/10.1002/cssc.201500334.
250. Senthil Kumar SM, et al. Hydrothermal assisted morphology designed MoS2 material as alternative cathode

catalyst for PEM electrolyser application. Int J Hydrog Energy. 2016;41(31):13331–40. https://doi.org/10.1016/j.ijhydene.2016.05.285.
251. Lu AY, et al. High-sulfur-vacancy amorphous molybdenum sulfide as a high current electrocatalyst in hydrogen evolution. Small. 2016;12(40):5530–7. https://doi.org/10.1002/smll.201602107.
252. Kim JH, Kim H, Kim J, Lee HJ, Jang JH, Ahn SH. Electrodeposited molybdenum sulfide as a cathode for proton exchange membrane water electrolyzer. J Power Sources. 2018;392(April):69–78. https://doi.org/10.1016/j.jpowsour.2018.04.087.
253. Di Giovanni C, et al. Low-cost nanostructured iron sulfide electrocatalysts for PEM water electrolysis. ACS Catal. 2016;6(4):2626–31. https://doi.org/10.1021/acscatal.5b02443.
254. Shiva Kumar S, Ramakrishna SUB, Rama Devi B, Himabindu V. Phosphorus-doped carbon nanoparticles supported palladium electrocatalyst for the hydrogen evolution reaction (HER) in PEM water electrolysis. Ionics (Kiel). 2018;24(10):3113–21. https://doi.org/10.1007/s11581-018-2471-0.
255. Ramakrishna SUB, Srinivasulu Reddy D, Shiva Kumar S, Himabindu V. Nitrogen doped CNTs supported Palladium electrocatalyst for hydrogen evolution reaction in PEM water electrolyser. Int J Hydrog Energy. 2016;41(45):20447–54. https://doi.org/10.1016/j.ijhydene.2016.08.195.
256. Shiva Kumar S, Ramakrishna SUB, Rama Devi B, Himabindu V. Phosphorus-doped graphene supported palladium (Pd/PG) electrocatalyst for the hydrogen evolution reaction in PEM water electrolysis. Int J Green Energy. 2018;15(10):558–67. https://doi.org/10.1080/15435075.2018.1508468.
257. Sun X, et al. Earth-abundant electrocatalysts in proton exchange membrane electrolyzers. Catalysts. 2018. https://doi.org/10.3390/catal8120657.
258. Lewinski KA, van der Vliet D, Luopa SM. NSTF advances for PEM electrolysis—the effect of alloying on activity of NSTF electrolyzer catalysts and performance of NSTF based PEM electrolyzers. ECS Trans. 2015;69(17):893–917. https://doi.org/10.1149/06917.0893ECST/XML.
259. Rozain C, Mayousse E, Guillet N, Millet P. Influence of iridium oxide loadings on the performance of PEM water electrolysis cells: Part I-Pure IrO2-based anodes. Appl Catal B. 2016;182:153–60. https://doi.org/10.1016/J.APCATB.2015.09.013.
260. Lettenmeier P, et al. Durable membrane electrode assemblies for proton exchange membrane electrolyzer systems operating at high current densities. Electrochim Acta. 2016;210:502–11. https://doi.org/10.1016/J.ELECTACTA.2016.04.164.
261. Maric R, Yu H. Proton exchange membrane water electrolysis as a promising technology for hydrogen production and energy storage. Nanostruct Energy Gener Transm Storage. 2019. https://doi.org/10.5772/intechopen.78339.
262. Ursúa A, Gandía LM, Sanchis P. Hydrogen production from water electrolysis: current status and future trends. Proc IEEE. 2012;100(2):410–26. https://doi.org/10.1109/JPROC.2011.2156750.
263. Choi B, Jung D, Lee J. Mechanical and electromagnetic analysis of high speed motor/generator for electric turbo compounding system. Open Electr Electron Eng J. 2018;12(1):121–31. https://doi.org/10.2174/1874129001812010121.
264. Öztaş EA, Berkay GE, Gülen S. Comparison of turbo compounding technoligies on gasoline and diesel engines. Int J Automot Eng Technol. 2023;12(1):22–9. https://doi.org/10.18245/ijaet.1175788.
265. Majaw T, Deka R, Roy S, Goswami B. Solar charge controllers using MPPT and PWM: a review. ADBU J Electr Electron Eng (AJEEE). 2018;2(1):1–4.
266. Deepika M (2023) MPPT-based charge controller for battery fast charging. In: 2023 9th international conference on advanced computing and communication systems (ICACCS), IEEE, pp 449–453. https://doi.org/10.1109/ICACCS57279.2023.10112852
267. Seekham P, Khongkrapan P, Tippayawong N. Performance enhancement of a hot air food dryer with infrared heating system. New York: AIP Publishing; 2022. p. 020076.
268. Antal T. Comparative study of three drying methods: freeze, hot air-assisted freeze and infrared-assisted freeze modes. Agron Res. 2015;13(4):863–78.
269. Shilpa MK, Abdul Raheman M, Aabid A, Baig M, Veeresha RK, Kudva N. A systematic review of thermoelectric peltier devices: applications and limitations. Fluid Dyn Mater Process. 2023;19(1):187–206. https://doi.org/10.32604/fdmp.2022.020351.
270. Ayers KE. Low temperature PEM cells leveraging hydrogen and oxygen evolution electrodes. ECS Meet Abstr. 2022;MA2022–02(46):1716–1716. https://doi.org/10.1149/MA2022-02461716mtgabs.
271. Lin HY, et al. Oxygen evolution electrocatalysts for the proton exchange membrane electrolyzer: challenges on stability. Small Methods. 2022. https://doi.org/10.1002/smtd.202201130.
272. Aly WIA, Abdo M, Bedair G, Hassaneen AE. Thermal performance of a diffusion absorption refrigeration system driven by waste heat from diesel engine exhaust gases. Appl Therm Eng. 2017;114:621–30. https://doi.org/10.1016/j.applthermaleng.2016.12.019.
273. Liu B, Huang B, Feng L, Raise A. Analysis of a high-performance polygeneration system for efficient waste heat recovery of an organic flash cycle: Multi-criteria analysis and optimization. Appl Therm Eng. 2022. https://doi.org/10.1016/j.applthermaleng.2022.118772.
274. Li M, Zhuang Y, Song M, Li W, Du J. Techno-economic and carbon footprint feasibility assessment for polygeneration process of carbon-capture coal-to-methanol/power and molten carbonate fuel cell. Energy Convers Manag. 2021. https://doi.org/10.1016/j.enconman.2021.114015.
275. Chen L, Lin J, Luo J, Sun F, Wu C. Friction effect on the characteristic performance of diesel engines. Int J Energy Res. 2002;26(11):965–71. https://doi.org/10.1002/er.820.
276. Fan FR, Tang W, Yao Y, Luo J, Zhang C, Wang ZL. Complementary power output characteristics of electromagnetic generators and triboelectric generators. Nanotechnology. 2014. https://doi.org/10.1088/0957-4484/25/13/135402.
277. Wang H, Torki M, Taherian A, Beigi M, Xiao HM, Fang XM. Analysis of exergetic performance for a combined ultrasonic power/convective hot air dryer. Renew Sustain Energy Rev. 2023. https://doi.org/10.1016/j.rser.2023.113607.
278. El-Mesery HS, Tolba NM, Kamel RM. Mathematical modelling and performance analysis of airflow distribution systems inside convection hot-air dryers. Alex Eng J. 2023;62:237–56. https://doi.org/10.1016/j.aej.2022.07.027.
279. He WF, Zhang XK, Han D, Gao L. Performance analysis of a water-power combined system with air-heated humidification dehumidification process. Energy. 2017;130:218–27. https://doi.org/10.1016/j.energy.2017.04.136.
280. Ghiasirad H, Asgari N, Khoshbakhti Saray R, Mirmasoumi S. Thermoeconomic assessment of a geothermal based combined cooling, heating, and power system, integrated with a humidification-dehumidification desalination unit and an absorption heat transformer. Energy Convers Manag. 2021. https://doi.org/10.1016/j.enconman.2021.113969.
281. Prasetyo SD, Prabowo AR, Arifin Z. The effect of collector design in increasing PVT performance: current state and

milestone. Mater Today Proc. 2022;63:S1–9. https://doi.org/10.1016/j.matpr.2021.12.356.
282. Abdul-Ganiyu S, Quansah DA, Ramde EW, Seidu R, Adaramola MS. Study effect of flow rate on flat-plate water-based photovoltaic-thermal (PVT) system performance by analytical technique. J Clean Prod. 2021. https://doi.org/10.1016/j.jclepro.2021.128985.
283. Hiwale AS, Patil MV, Vinchurkar H. An efficient MPPT solar charge controller. Int J Adv Res Electr Electron Instrum Eng. 2014;3(7):10505–11. https://doi.org/10.15662/ijareeie.2014.0307017.
284. Liu Y, Wang Y, Wang M, Xu Z, Peng Y, Li M. Coordinated VSG control of photovoltaic/battery system for maximum power output and grid supporting. IEEE J Emerg Sel Top Circuits Syst. 2022;12(1):301–9. https://doi.org/10.1109/JETCAS.2022.3143716.
285. Zhang X, Chen X, Lin B, Chen J. Maximum equivalent efficiency and power output of a PEM fuel cell/refrigeration cycle hybrid system. Int J Hydrog Energy. 2011;36(3):2190–6. https://doi.org/10.1016/j.ijhydene.2010.11.088.
286. Ratlamwala TAH, El-Sinawi AH, Gadalla MA, Aidan A. Performance analysis of a new designed PEM fuel cell. Int J Energy Res. 2012;36(11):1121–32. https://doi.org/10.1002/er.1877.
287. Vijay Babu AR, Manoj Kumar P, Srinivasa Rao G. Parametric study of the proton exchange membrane fuel cell for investigation of enhanced performance used in fuel cell vehicles. Alex Eng J. 2018;57(4):3953–8. https://doi.org/10.1016/j.aej.2018.03.010.
288. Demir ME, Dincer I. Development of a hybrid solar thermal system with TEG and PEM electrolyzer for hydrogen and power production. Int J Hydrog Energy. 2017;42(51):30044–56. https://doi.org/10.1016/j.ijhydene.2017.09.001.
289. Vives AM, Wang R, Roy S, Smallbone A. Techno-economic analysis of large-scale green hydrogen production and storage. Appl Energy. 2023. https://doi.org/10.1016/j.apenergy.2023.121333.
290. Edwards S, Eitel J, Pantow E, Geskes P, Lutz R, Tepas J. Waste heat recovery the next challenge for commercial vehicle thermomanagement. SAE Int J Commer Veh. 2012;5(1):2012–1205.
291. Sprouse C, Depcik C. Review of organic Rankine cycles for internal combustion engine exhaust waste heat recovery. Appl Therm Eng. 2013;51(1–2):711–22. https://doi.org/10.1016/j.applthermaleng.2012.10.017.
292. Orr B, Akbarzadeh A, Mochizuki M, Singh R. A review of car waste heat recovery systems utilising thermoelectric generators and heat pipes. Appl Therm Eng. 2016;101:490–5. https://doi.org/10.1016/j.applthermaleng.2015.10.081.
293. Wahile GS, Malwe PD, Kolhe AV. Waste heat recovery from exhaust gas of an engine by using a phase change material. Mater Today Proc. 2020;28:2101–7. https://doi.org/10.1016/j.matpr.2020.03.247.
294. Haidar JG, Ghojel JI. Waste heat recovery from the exhaust of low-power diesel engine using thermoelectric generators. Int Conf Thermoelectr ICT Proc. 2001. https://doi.org/10.1109/ICT.2001.979919.
295. Park T, Teng H, Hunter GL, van der Velde B, Klaver J (2011) A rankine cycle system for recovering waste heat from hd diesel engines—experimental results. https://doi.org/10.4271/2011-01-1337
296. Singh DV, Pedersen E. A review of waste heat recovery technologies for maritime applications. Energy Convers Manag. 2016;111:315–28. https://doi.org/10.1016/j.enconman.2015.12.073.
297. Nadaf SL, Gangavati PB. A review on waste heat recovery and utilization from diesel engines. Int J Adv Eng Technol. 2014;31:39–45.
298. Karvonen M, Kapoor R, Uusitalo A, Ojanen V. Technology competition in the internal combustion engine waste heat recovery: a patent landscape analysis. J Clean Prod. 2016;112:3735–43. https://doi.org/10.1016/j.jclepro.2015.06.031.
299. Christodoulides P, Agathokleous R, Aresti L, Kalogirou SA, Tassou SA, Florides GA. Waste heat recovery technologies revisited with emphasis on new solutions, including heat pipes, and case studies. Energies (Basel). 2022;15(1):384. https://doi.org/10.3390/en15010384.
300. Hoang AT. Waste heat recovery from diesel engines based on organic rankine cycle. Appl Energy. 2018;231:138–66.
301. Ahmed SF, Rafa N, Mehnaz T, Ahmed B, Islam N, Mofijur M, Shafiullah GM. Integration of phase change materials in improving the performance of heating, cooling, and clean energy storage systems: an overview. J Clean Prod. 2022;364:132639.
302. Subramanian M, Hoang AT, Kalidasan B, Nižetić S, Solomon JM, Balasubramanian D, Nguyen XP. A technical review on composite phase change material based secondary assisted battery thermal management system for electric vehicles. J Clean Prod. 2021;322:129079.